lectin (*Mincle*; also called *Clec4e* and *Clecsf9*), a type II transmembrane C-type lectin, is induced selectively in macrophages during the interaction between adipocytes and macrophages. Mincle originally was identified as a transcriptional target of CCAAT/enhancer binding protein β in macrophages in response to proinflammatory stimuli such as LPS, TNF-α, IL-6, and IFN-γ (10). Our data also suggest that Mincle is induced in M1 macrophages in the adipose tissue in obesity through the saturated fatty acid/TLR4/NF-κB pathway. This study is the first detailed analysis of a C-type lectin in adipose tissue macrophages, thereby providing a novel insight into the molecular mechanism underlying adipose tissue inflammation.

RESEARCH DESIGN AND METHODS

Reagents. LPS (from *Escherichia coli* O111: B4) and BAY11-7085, an NF-κB inhibitor, were purchased from Sigma (San Diego, CA) and Merck (Whitehouse Station, NJ), respectively. Palmitate and oleate were purchased from Sigma, solubilized in ethanol, and conjugated with fatty acid- and immunoglobulin-free BSA (Sigma) at a molar ratio of 10 to 1 (fatty acids to BSA) in a low-serum medium as described (7). The concentrations of palmitate and oleate used in this study (<200 μmol/L) were within the physiologic range. All other reagents were purchased from Sigma or Nacalai Tesque (Kyoto, Japan), unless otherwise described.

Animals. Male C3H/HeJ (HeJ) mice, which have defective LPS signaling attributed to a missense mutation in the *TLR4* gene (11), and control C3H/HeN (HeN) mice were purchased from CLEA Japan (Tokyo, Japan). Male C57BL/6 J leptin-deficient *ob/ob* mice and their wild-type littermates were purchased from Charles River Japan (Tsukuba, Japan). The animals were housed in individual cages in a temperature-, humidity-, and light-controlled room (12-h light and 12-h dark cycle) and were allowed free access to water and standard diet (Oriental MF; 362 kcal/100 g, 5.4% energy as fat; Oriental Yeast, Tokyo, Japan), unless otherwise noted. In some experiments, mice were given free access to water and either the standard diet (SD) or the high-fat diet (HFD) (D12492; 556 kcal/100 g, 60% energy as fat; Research Diets, New Brunswick, NJ) for 16 weeks. All animal experiments were conducted according to the guidelines of the Tokyo Medical and Dental University Committee on Animal Research (no. 100098).

Cell culture. The RAW264 macrophage cell line (Riken BioResource Center, Tsukuba, Japan) and 3T3-L1 preadipocytes (American Type Culture Collection, Manassas, VA) were maintained in Dulbecco's modified Eagle's medium (Nacalai Tesque) containing 10% FBS (7,8). Generation of RAW264 macrophages overexpressing a superrepressor form of the inhibitor of κB (IκB)-α (SR-IκBα; a degradation-resistant mutant of IκBα) were reported previously (9,12,13). Peritoneal and bone-marrow–derived macrophages were prepared as described (8,14,15). For macrophage polarization experiments, bone-marrow cell (BMC)-derived macrophages were cultured for 24 h in Iscove's modified Dulbecco's medium (Invitrogen, Carlsbad, CA) containing 5% FBS supplemented with 10 ng/mL LPS and 20 ng/mL IFN-γ (for M1 polarization) or 10 ng/mL IL-4 (for M2 polarization) (5). Control macrophages were prepared in Iscove's modified Dulbecco's medium containing 5% FBS alone.

Coculture of adipocytes and macrophages. Coculture of 3T3-L1 adipocytes and macrophages (RAW264 or peritoneal macrophages) in the contact system was performed as described (7,8). In brief, serum-starved differentiated 3T3-L1 adipocytes (~0.5×10^6 cells) were cultured in a 35-mm dish, and macrophages (1.0×10^5 cells) were plated onto 3T3-L1 adipocytes (contact coculture) (Fig. 1*A*). The cells were cultured with direct cell-to-cell contact and harvested after a 24-h incubation, unless otherwise described. As a control (control culture), adipocytes and macrophages, the numbers of which were equal to those in the coculture, were cultured separately and mixed after harvest. Our previous data suggest that there is no apparent difference in macrophage cell number between the coculture and control culture (7).

In some experiments, we cocultured RAW264 macrophages with adipose tissue explants in the transwell system, in which adipose tissue explants of 8-week-old C57BL/6 J mice were plated in a transwell insert with a 0.4-μm porous membrane (Corning, Corning, NY) to separate them from RAW264 macrophages (Supplementary Fig. 1*A*). After incubation for 8 h, RAW264 macrophages in the lower well were harvested.

cDNA microarray analysis. cDNA microarray analysis was performed using mouse genome 430A 2.0 (Affymetrix, Santa Clara, CA) as described (8,9). Total RNA was prepared from the contact coculture of 3T3-L1 adipocytes and RAW264 macrophages, the control culture, and 3T3-L1 adipocytes alone (Fig. 1*A*). In this experiment, we cocultured the cells for 8 h. We also performed a hierarchical clustering analysis using GeneSpring (Agilent Technologies, Palo Alto, CA).

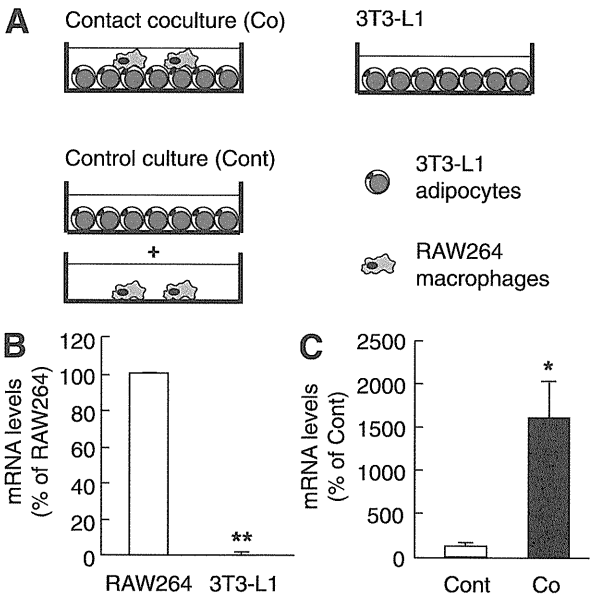

FIG. 1. Identification of *Mincle* as a target gene upregulated in the coculture of 3T3-L1 adipocytes and RAW264 macrophages. *A*: Illustration of the contact coculture system composed of 3T3-L1 adipocytes and RAW264 macrophages. *B*: Mincle mRNA expression in RAW264 and 3T3-L1. *C*: Effect of coculture on Mincle mRNA expression. $n = 4$. *$P < 0.05$; **$P < 0.01$.

Quantitative real-time PCR. Total RNA was extracted from various tissues and cultured cells using a TRIzol reagent (Invitrogen), and quantitative real-time PCR was performed with an ABI Prism 7000 Sequence Detection System using PCR Master Mix reagent (Applied Biosystems, Foster City, CA) as described (7–9). Primers used to detect mouse and human mRNAs are described in Supplementary Tables 1 and 2, respectively. Levels of mRNA were normalized to those of 36B4 mRNA (for mouse) or β-actin (for humans).

Preparation of rabbit polyclonal anti-mouse Mincle antibody and Western blot analysis. Details are shown in the Supplementary Research Design and Methods.

Human studies on Mincle expression in the adipose tissue and circulating monocytes. Details are shown in Supplementary Research Design and Methods and Supplementary Table 3. The study protocol was approved by the ethical committee on human research of The University of Tokushima Graduate School, Kyoto Medical Center, and the Tokyo Medical and Dental University.

Statistical analysis. Data were expressed as the means ± SE. Statistical analysis was performed using ANOVA. $P < 0.05$ was considered to be statistically significant. In the human study, linear regression analysis was used to evaluate the relationship between Mincle mRNA levels and BMI.

RESULTS

Coculture-induced Mincle mRNA expression in macrophages. To screen the gene(s) that are upregulated selectively in macrophages during the interaction between adipocytes and macrophages, we performed cDNA microarray analysis of the coculture of 3T3-L1 adipocytes and RAW264 macrophages in the contact system (Fig. 1*A*). There were 316 genes upregulated (>1.5-fold) in the coculture of 3T3-L1 adipocytes and RAW264 macrophages relative to the control culture, including chemokines, proinflammatory cytokines, and acute-phase reactants (Supplementary Table 4). We also compared the control culture with 3T3-L1 adipocytes alone to examine macrophage selective expression (Supplementary Table 4). In this study, we have focused on Mincle, a type II transmembrane C-type

lectin in macrophages, for the following reasons. First, Mincle is induced by LPS (10). Second, Mincle is selectively expressed in macrophages (Supplementary Table 4). We confirmed by real-time PCR that Mincle exhibits highly selective expression in RAW264 macrophages relative to 3T3-L1 adipocytes and is markedly upregulated by the coculture ($P < 0.01$ and $P < 0.05$) (Fig. 1*B* and *C*, respectively). Last, Mincle acts as a pathogen sensor to induce proinflammatory cytokine and chemokine expression such as TNF-α and macrophage inflammatory protein 2 (16–19). Indeed, cluster analysis revealed that Mincle shows a similar expression pattern with eight genes (Supplementary Fig. 2), which are all related to inflammatory responses. These observations, taken together, suggest that Mincle is selectively induced in macrophages during the interaction between adipocytes and macrophages.

Role of the saturated fatty acid/TLR4/NF-κB pathway in Mincle expression. Because saturated fatty acids are a major adipocyte-derived paracrine mediator of inflammation in macrophages (8,20), we examined the effect of palmitate, a major saturated fatty acid released from 3T3-L1 adipocytes, on Mincle mRNA expression in RAW264 or peritoneal macrophages. Treatment with palmitate for 24 h induced Mincle mRNA and protein expression in RAW264 macrophages in a dose-dependent manner (Fig. 2*A–C*). On the other hand, there was no apparent change in Mincle mRNA and protein expression when it was treated with unsaturated fatty acid oleate (Fig. 2*A–C*). We also found that palmitate, as well as LPS, induces Mincle mRNA expression in peritoneal macrophages of control C3H/HeN mice. Importantly, the induction was markedly inhibited in peritoneal macrophages of TLR4 signal–deficient C3H/HeJ mice ($P < 0.01$) (Fig. 2*D*). Moreover, treatment with BAY11-7085, an NF-κB inhibitor, significantly inhibited the palmitate-induced Mincle mRNA expression in RAW264 macrophages ($P < 0.05$) (Fig. 2*E*). The palmitate-induced Mincle mRNA expression also was significantly reduced in RAW264 macrophages overexpressing SR-IκBα, a dominant-negative form of IκBα, relative to those without SR-IκBα expression ($P < 0.01$) (Fig. 2*F*). These observations suggest that the TLR4/NF-κB pathway is involved in the saturated fatty acid–induced Mincle expression in macrophages.

To elucidate the role of TLR4 in the coculture-induced Mincle mRNA expression, we performed the coculture of 3T3-L1 adipocytes and peritoneal macrophages of C3H/HeJ or C3H/HeN mice. Coculture of 3T3-L1 adipocytes with C3H/HeN peritoneal macrophages resulted in the marked upregulation of Mincle mRNA, which was significantly inhibited in the coculture with C3H/HeJ peritoneal macrophages ($P < 0.05$) (Fig. 2*G*). Moreover, treatment with BAY11-7085 effectively inhibited the coculture-induced Mincle mRNA expression ($P < 0.05$) (Fig. 2*H*). These observations, taken together, suggest the role of the TLR4/NF-κB pathway in the coculture-induced Mincle mRNA expression.

Mincle expression in adipose tissue of obese mice. Because there is no previous report on the tissue distribution of Mincle expression in vivo, we next examined the tissue distribution of Mincle mRNA in genetically obese *ob/ob* mice and wild-type mice (Fig. 3*A*). Real-time PCR analysis revealed that Mincle mRNA is expressed most abundantly in the spleen of lean wild-type mice. Other organs such as the liver, colon, intestine, and adipose tissue also expressed Mincle mRNA, although to a lesser extent than in the spleen. Similar to macrophage marker F4/80 and M1 macrophage marker CD11c, Mincle mRNA expression was markedly increased in the adipose tissue of *ob/ob* mice relative to wild-type mice. We also observed a significant upregulation of Mincle mRNA in the adipose tissue of diet-induced obese mice ($P < 0.01$) (Fig. 3*B*). Collagenase digestion of adipose tissue, which is validated by F4/80 and adiponectin mRNA expression (9), revealed that Mincle mRNA expression is predominantly detected in the stromal-vascular fraction, which was markedly increased in *ob/ob* mice relative to wild-type mice ($P < 0.05$) (Fig. 3*C*). In this study, there was a significant increase in Mincle mRNA expression in the heart and liver ($P < 0.01$ and $P < 0.05$, respectively) (Fig. 3*A*). These observations, taken together, suggest that Mincle is markedly upregulated mostly in adipose tissue macrophages in obesity.

Role of TLR4 in obesity-induced Mincle mRNA expression in vivo. Using C3H/HeJ and C3H/HeN mice fed an HFD or an SD for 16 weeks, we examined the involvement of TLR4 signaling in obesity-induced Mincle mRNA expression in vivo. We previously demonstrated that the weight gain of C3H/HeJ mice as a result HFD feeding is roughly comparable with that of C3H/HeN mice (9,21). We also found that there is no appreciable difference in the number of F4/80-positive macrophages between the genotypes (9,21). In this study, Mincle mRNA expression in adipose tissue on an HFD was significantly attenuated in C3H/HeJ mice relative to C3H/HeN mice ($P < 0.05$), whereas there was no appreciable difference between the genotypes on an SD (Fig. 4*A*). Similarly, mRNA expression of the M1 macrophage marker, CD11c, tended to be decreased in the adipose tissue of C3H/HeJ mice relative to C3H/HeN mice, although CD11c mRNA expression was significantly increased on an HFD relative to an SD in both genotypes (Fig. 4*B*). These observations suggest that TLR4 signaling plays an important role in the obesity-induced Mincle mRNA expression in adipose tissue macrophages in vivo.

Mincle mRNA expression in BMC-derived M1 macrophages in vitro. To further explore Mincle mRNA expression in M1 versus M2 macrophages, we examined Mincle mRNA expression in BMC-derived M1 and M2 macrophages in vitro. We confirmed that TNF-α and inducible nitric oxide (NO) synthase mRNAs are expressed exclusively in BMC-derived M1 macrophages (Fig. 5*A*), whereas BMC-derived M2 macrophages show substantial expression of arginase 1 and mannose receptor mRNAs (Fig. 5*B*). In this study, Mincle mRNA was predominantly expressed in BMC-derived M1 macrophages (Fig. 5*C*). In contrast, no appreciable amount of Mincle mRNA was detected in BMC-derived M2 macrophages (Fig. 5*C*). These observations suggest that Mincle is expressed in M1 macrophages rather than in M2 macrophages in vitro.

Mincle mRNA expression in the adipose tissue and circulating monocytes of obese subjects. We also examined Mincle mRNA expression in human subcutaneous adipose tissue. We did not observe significant differences in blood pressure and serum triglycerides, HDL cholesterol, LDL cholesterol, and HbA_{1c} levels between the groups (Table 1). On the other hand, there was a tendency of increased expression of CD11c and CD68 mRNAs in the adipose tissue of obese subjects relative to nonobese subjects (Fig. 6*A*). In this study, Mincle mRNA expression was markedly increased in the adipose tissue of obese subjects relative to nonobese subjects ($P < 0.01$) (Fig. 6*A*). Linear regression analysis also revealed a significantly positive correlation between Mincle mRNA levels and BMI ($r^2 = 0.3589$, $P < 0.01$) (Fig. 6*B*).

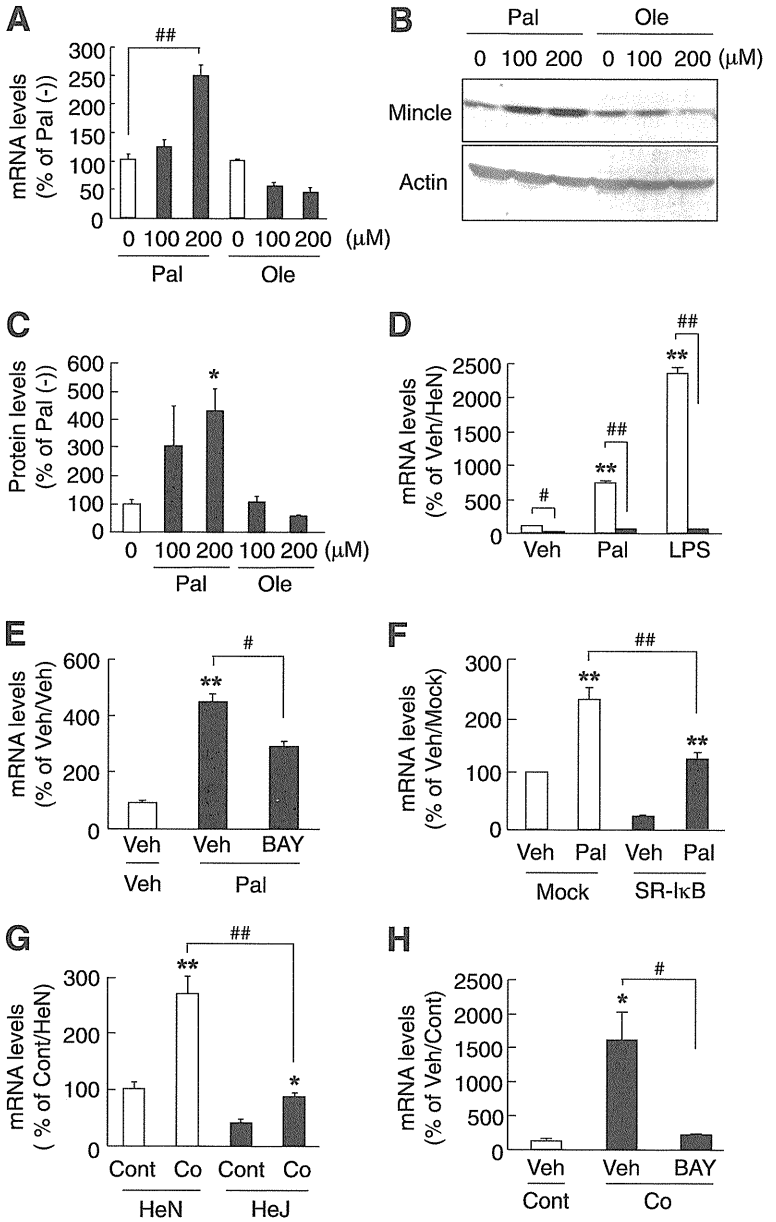

FIG. 2. Effect of palmitate on Mincle expression in cultured macrophages. *A–C*: Effect of palmitate (Pal) and oleate (Ole) on Mincle mRNA (*A*) and protein (*B* and *C*) expression in RAW264 macrophages. Representative Western blots (*B*) and quantitative relative protein expression (*C*) of Mincle. *D*: Mincle mRNA expression stimulated by palmitate (200 μmol/L) and LPS (10 ng/mL) in peritoneal macrophages prepared from TLR4 signal–deficient C3H/HeJ (■, HeJ) and control C3H/HeN (□, HeN) mice. *E*: Effect of BAY11-7085 (BAY; an NF-κB inhibitor) on the palmitate-induced Mincle mRNA expression in RAW264 macrophages. *F*: Effect of palmitate on Mincle mRNA expression in SR-IκBα- (a dominant-negative form of IκBα) and mock-overexpressing RAW264 (SR-IκB and Mock, respectively) macrophages. *G*: Effect of coculture of 3T3-L1 adipocytes and peritoneal macrophages of C3H/HeJ and C3H/HeN mice on Mincle mRNA expression. *H*: Effect of BAY (1 μmol/L) on coculture-induced Mincle mRNA expression. Co, coculture; Cont, control culture; Veh, vehicle. n = 3–4. *$P < 0.05$; **$P < 0.01$ vs. each control; #$P < 0.05$; ##$P < 0.01$.

We further examined Mincle mRNA expression in circulating monocytes of nondiabetic subjects. We did not observe significant differences in diastolic blood pressure and serum lipid levels between the groups, whereas systolic blood pressure was significantly high in obese subjects relative to nonobese subjects ($P < 0.05$) (Supplementary Table 3). In this study, Mincle mRNA expression was significantly increased in the circulating monocytes of obese subjects relative to nonobese subjects ($P < 0.05$) (Fig. 7). In this setting, circulating monocytes of obese subjects exhibited higher TNF-α and IL-6 mRNA expression and lower IL-10 mRNA expression than those of nonobese subjects (Fig. 7). Collectively, these observations suggest that Mincle expression is increased in the adipose tissue and circulating monocytes in obese subjects.

DISCUSSION

During the course of adipose tissue remodeling in obesity, infiltrating macrophages may participate in the inflammatory pathways that are activated in the adipose tissue (1,2,7).

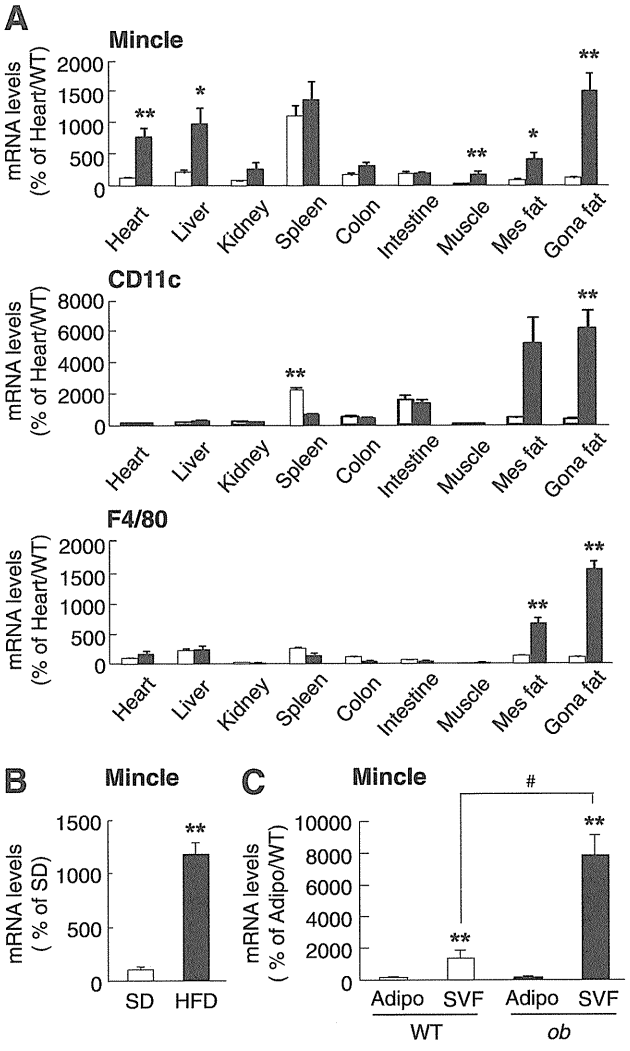

FIG. 3. Mincle mRNA expression in mouse adipose tissue. *A*: Tissue distribution of Mincle (*top*), M1 macrophage marker CD11c (*middle*), and macrophage marker F4/80 (*bottom*) mRNAs in wild-type (WT) mice (□) and *ob/ob* mice (■). *$P < 0.05$; **$P < 0.01$ vs. the respective wild-type mice. *B*: Mincle mRNA expression in the adipose tissue of diet-induced obese mice. **$P < 0.01$ vs. SD. *C*: Mincle mRNA expression in mature adipocytes (Adipo) and stromal-vascular fraction (SVF) in the adipose tissue of wild-type mice (WT) and *ob/ob* mice (*ob*). $n = 4$–6. **$P < 0.01$ vs. each adipocyte; #$P < 0.05$.

Using an in vitro coculture system composed of 3T3-L1 adipocytes and RAW264 macrophages, we have provided evidence that saturated fatty acids, which are released in large quantities from hypertrophied adipocytes via the macrophage-induced adipocyte lipolysis, serve as a naturally occurring ligand for TLR4 complex in macrophages, thereby aggravating chronic inflammatory changes in the adipose tissue in obesity (7,8). To understand the molecular mechanisms underlying the interaction between adipocytes and macrophages, it is therefore important to characterize molecules and pathways activated in macrophages in response to saturated fatty acids. Through a combination of cDNA microarray analyses of coculture of 3T3-L1 adipocytes and RAW264 macrophages, we have identified several candidate genes that are induced in macrophages during the interaction between adipocytes and macrophages.

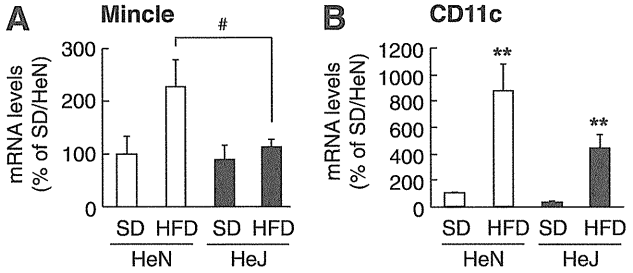

FIG. 4. Role of TLR4 in obesity-induced Mincle mRNA expression in mouse adipose tissue. Mincle (*A*) and CD11c (*B*) mRNA expression in the adipose tissue of C3H/HeN and C3H/HeJ mice fed an SD or an HFD. $n = 4$. **$P < 0.01$ vs. each SD; #$P < 0.05$.

Because there are no previous reports on the role of Mincle in obesity-induced adipose tissue inflammation, it is interesting to speculate that Mincle plays a novel role in the pathophysiology of obesity and obesity-related metabolic derangements.

This study provides in vitro evidence that saturated fatty acids induce Mincle mRNA expression in macrophages at least partly through the TLR4/NF-κB pathway. This is consistent with a previous report that the 5′-flanking region of the mouse *Mincle* gene has a couple of putative binding motifs for NF-κB (10). We also demonstrate with a series of coculture experiments that the TLR4/NF-κB pathway is involved in the coculture-induced Mincle mRNA expression. In this study, we observed that Mincle mRNA expression is significantly increased in RAW264 macrophages in the transwell coculture system as well as the contact coculture system, supporting the role of adipocyte-derived secretory factors, such as saturated fatty acids, in the induction of Mincle expression. On the other hand, it seems that the upregulation of Mincle expression by treatment with palmitate or in the transwell coculture system is apparently modest relative to that in the contact coculture system. It is therefore conceivable that in addition to secretory factors, direct contact between adipocytes and macrophages also is involved in the induction of Mincle expression in the contact coculture system. On the other hand, there still appears to be some upregulation of Mincle expression in the absence of TLR4 signaling in coculture using HeJ peritoneal macrophages. Indeed, Matsumoto et al. (10) reported that Mincle mRNA expression is markedly induced in macrophages in response to proinflammatory cytokines such as TNF-α, IL-6, and IFN-γ. It is interesting to identify other adipocyte-derived paracrine signals than saturated fatty acids, which are involved in the coculture-induced Mincle expression in macrophages.

In this study, we demonstrate that Mincle mRNA expression is markedly induced in the stromal-vascular fraction in the adipose tissue of obese mice, suggesting the predominant expression of Mincle in adipose tissue macrophages in vivo. The obesity-induced Mincle mRNA expression is markedly attenuated in the adipose tissue of C3H/HeJ mice relative to C3H/HeN mice, suggesting the involvement of TLR4 signaling in vivo. There is considerable evidence that macrophages, which are infiltrated into the adipose tissue in obesity, exhibit the phenotypic change from anti-inflammatory M2 to proinflammatory M1 polarization (6). Given that Mincle is induced in macrophages in response to LPS (10), an important mediator of M1 macrophage polarization in vitro (5), it is conceivable that Mincle is expressed in M1 macrophages rather than in

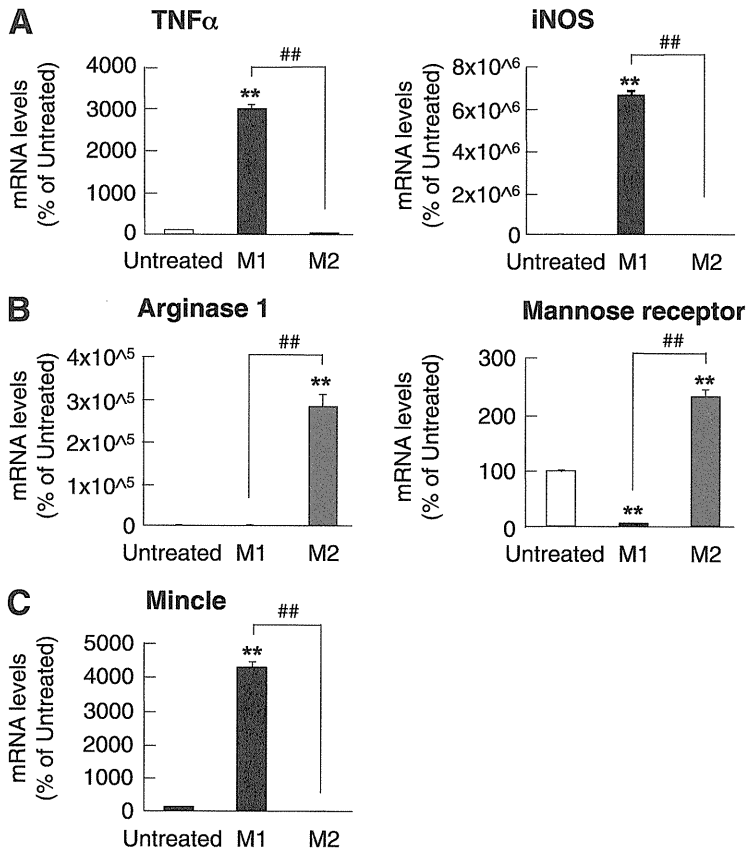

FIG. 5. Mincle mRNA expression in M1 and M2 macrophages in vitro. mRNA expression of M1 markers (TNF-α and inducible NO synthase [iNOS]) (*A*), M2 markers (arginase 1 and mannose receptor) (*B*), and Mincle (*C*) in BMC-derived macrophages. M1, M1 polarization with 100 ng/mL LPS and 20 ng/mL IFN-γ; M2, M2 polarization with 10 ng/mL of IL-4. $n = 4$. **$P < 0.01$ vs. untreated; ##$P < 0.01$.

M2 macrophages. In this study, obesity-induced CD11c mRNA expression tends to be reduced in the adipose tissue of C3H/HeJ mice relative to C3H/HeN mice, suggesting the role of TLR4 signaling in M1 macrophage polarization in vivo. We also found that Mincle mRNA expression is attenuated in parallel with CD11c mRNA expression in HFD-fed C3H/HeJ mice relative to HFD-fed C3H/HeN mice. Given their critical role as a major adipocyte-derived paracrine mediator of inflammation in macrophages (7), it is likely that saturated fatty acids, when released from adipocytes, are an endogenous ligand that induces Mincle mRNA expression in macrophages at least partly through the TLR4/NF-κB pathway in vivo. These observations, taken together, suggest that Mincle is induced in M1 macrophages in adipose tissue through TLR4 signaling in obesity. This concept is supported by our in vitro observation that Mincle mRNA is expressed in BMC-derived M1 macrophages rather than in BMC-derived M2 macrophages.

TABLE 1
Clinical characteristics and metabolic parameters

	BMI <25 kg/m^2 group (nonobese)	BMI ≥25 kg/m^2 group (obese)
n	12	11
Age	66.9 ± 3.5	62.2 ± 3.6
BMI (kg/m^2)	22.9 ± 0.4	27.4 ± 0.7*
Systolic blood pressure (mmHg)	136 ± 7	127 ± 4
Diastolic blood pressure (mmHg)	71.6 ± 7.1	74.1 ± 3.1
Serum triglyceride concentration (mg/dL)	127 ± 16	153 ± 35
Serum HDL cholesterol (mg/dL)	43.6 ± 2.1	38.9 ± 3.4
Serum LDL cholesterol (mg/dL)	105 ± 12	85 ± 7
HbA_{1c} (%)	6.3 ± 0.3	6.4 ± 0.3

Data are means ± SE. *$P < 0.01$.

In this study, we also found that Mincle mRNA expression is increased in the adipose tissue of obese subjects relative to nonobese subjects. Moreover, there is a significant correlation between Mincle mRNA expression in adipose tissue and BMI. Because there may be species differences in adipose tissue macrophages between humans and rodents, the M1/M2 paradigm of murine adipose tissue macrophages (6) may not be entirely applicable to humans (22–24). Nevertheless, our data suggest that Mincle is expressed in proinflammatory macrophages in the adipose tissue of humans and mice. Moreover, we have shown that Mincle mRNA levels in circulating monocytes are significantly increased in obese subjects relative to nonobese subjects. Although monocytes are considered not fully differentiated cell types, recent studies showed

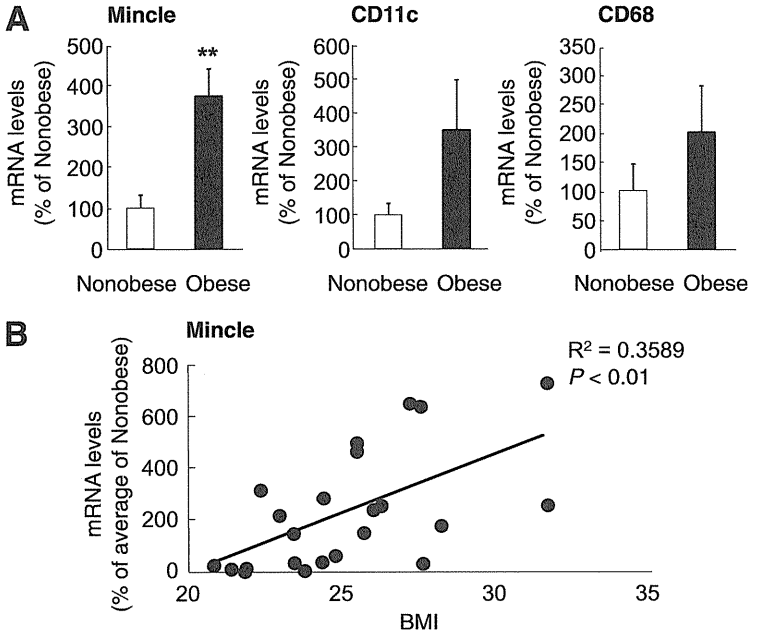

FIG. 6. Mincle mRNA expression in human adipose tissue. *A*: **mRNA expression of Mincle, CD11c, and CD68 in the subcutaneous adipose tissue of nonobese (BMI <25 kg/m^2, n = 12) and obese (BMI ≥25 kg/m^2, n = 11) subjects.** *B*: **Linear regression analysis of correlations between adipose Mincle mRNA expression and BMI. **P < 0.01.**

that circulating monocytes give rise to tissue macrophages and that monocyte subsets seem to reflect developmental stages of tissue macrophages (25). These observations support the notion that Mincle is overexpressed in adipose tissue macrophages in obese subjects relative to nonobese subjects. Additional studies are needed to elucidate the polarization state of adipose tissue macrophages expressing Mincle in humans. In this study, we do not exclude the possibility that differences in medication affect Mincle expression in the adipose tissue and circulating monocytes because obese subjects received more medication than nonobese subjects. On the other hand, serum free fatty acids (FFAs) are largely derived from adipose tissue, suggesting that the local FFA concentrations in adipose tissue are quite high relative to the serum FFA concentrations. It would be interesting to know the local concentrations of FFAs, especially saturated fatty acids, in the adipose tissue in obesity.

In the danger signal hypothesis (26,27), dying cells or damaged tissues are thought to release endogenous danger signals, which are recognized by innate immune receptors. We have shown that saturated fatty acids, which are released from adipocytes in response to a macrophage-derived death signal TNF-α, act as a naturally occurring ligand for the TLR4 complex to induce macrophage activation (8,28). It is therefore conceivable that saturated fatty acids also act as an endogenous danger signal that reports the dysfunctional state of hypertrophied adipocytes to adipose tissue macrophages in obesity. Sustained stimulation of other pathogen sensors expressed in macrophages by their endogenous ligands released from adipocytes should lead to chronic/homeostatic inflammatory responses, ranging from the basal homeostatic state to diseased tissue remodeling, which has been referred to as "homeostatic inflammation" (4). Recent studies (16–19) with Mincle-deficient mice demonstrated that Mincle serves as a pathogen sensor against certain types of fungi and bacteria and induces chemokine and proinflammatory cytokine production, suggesting that Mincle plays a critical role in immune responses to pathogens. On the other hand, Yamasaki et al. (29) reported that Mincle serves as a receptor for SAP130, a component of small, nuclear ribonucloprotein released from damaged cells, to sense

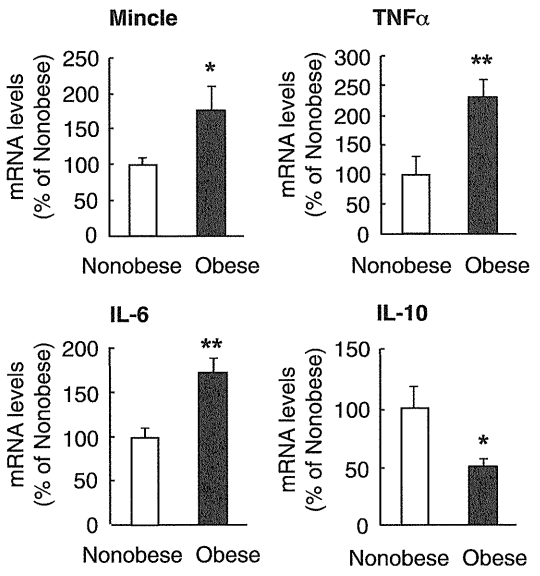

FIG. 7. Mincle mRNA expression in human circulating monocytes. mRNA expression of Mincle, TNF-α, IL-6, and IL-10 in circulating CD14-positive cells or monocytes of nonobese (BMI <25 kg/m^2, n = 25) and obese (BMI ≥25 kg/m^2, n = 25) subjects. *P < 0.05; **P < 0.01.

cell death and induce proinflammatory cytokine production. Recent evidence (30,31) suggests that dead adipocytes are surrounded by macrophages (or crown-like structure) in the adipose tissue of obese humans and mice. Collectively, Mincle may play a role in sensing adipocyte death to induce proinflammatory cytokine production in the adipose tissue in obesity. Moreover, there are two previous reports (32,33) that showed that some members of the immunoglobulin-like lectin family can modulate the inflammatory response through TLRs on immune cells. It is, therefore, tempting to speculate that endogenous ligand(s) for Mincle, in concert with saturated fatty acids, report the adipose tissue state to macrophages during the course of adipose tissue remodeling and induce inflammatory cytokine production. Additional studies are required to elucidate the pathophysiologic role of Mincle in obesity-induced adipose tissue inflammation.

In conclusion, we demonstrate that Mincle is induced selectively in macrophages during the interaction between adipocytes and macrophages in vitro and markedly increased in the adipose tissue of obese mice and humans in vivo. Our data also suggest that Mincle is expressed in M1 macrophages in the adipose tissue in obesity through the TLR4/NF-κB pathway. This study is the first detailed analysis of Mincle in adipose tissue macrophages, thereby providing a novel insight into the molecular mechanism underlying adipose tissue remodeling.

ACKNOWLEDGMENTS

This work was supported in part by grants-in-aid for scientific research from the Ministry of Education, Culture, Sports, Science, and Technology of Japan and the Ministry of Health, Labour, and Welfare of Japan; and research grants from Takeda Science Foundation, Ono Medical Research Foundation, Japan Vascular Disease Research Foundation, Yamaguchi Endocrine Research Foundation, and The Naito Foundation. No other potential conflicts of interest relevant to this article were reported.

M.I. researched data, contributed to discussion, and wrote the manuscript. T.S. researched data, contributed to discussion, and wrote, reviewed, and edited the manuscript. N.T. researched data and contributed to discussion. I.S., Y.H., N.S.-A., and Y.S. researched data. M.T. researched data and contributed to discussion. M.K.-S. and Y.M. researched data. Y.K. and M.S. contributed to discussion and reviewed and edited the manuscript. Y.O. contributed to discussion and wrote, reviewed, and edited the manuscript.

The authors thank Ai Togo (Tokyo Medical and Dental University) for secretarial assistance and Yousuke Sasaki (Kyoto Medical Center) for technical assistance.

REFERENCES

1. Weisberg SP, McCann D, Desai M, Rosenbaum M, Leibel RL, Ferrante AW Jr. Obesity is associated with macrophage accumulation in adipose tissue. J Clin Invest 2003;112:1796–1808
2. Hotamisligil GS. Inflammation and metabolic disorders. Nature 2006;444:860–867
3. Berg AH, Scherer PE. Adipose tissue, inflammation, and cardiovascular disease. Circ Res 2005;96:939–949
4. Suganami T, Ogawa Y. Adipose tissue macrophages: their role in adipose tissue remodeling. J Leukoc Biol 2010;88:33–39
5. Martinez FO, Gordon S, Locati M, Mantovani A. Transcriptional profiling of the human monocyte-to-macrophage differentiation and polarization: new molecules and patterns of gene expression. J Immunol 2006;177:7303–7311
6. Lumeng CN, Bodzin JL, Saltiel AR. Obesity induces a phenotypic switch in adipose tissue macrophage polarization. J Clin Invest 2007;117:175–184
7. Suganami T, Nishida J, Ogawa Y. A paracrine loop between adipocytes and macrophages aggravates inflammatory changes: role of free fatty acids and tumor necrosis factor α. Arterioscler Thromb Vasc Biol 2005;25:2062–2068
8. Suganami T, Tanimoto-Koyama K, Nishida J, et al. Role of the Toll-like receptor 4/NF-kappaB pathway in saturated fatty acid-induced inflammatory changes in the interaction between adipocytes and macrophages. Arterioscler Thromb Vasc Biol 2007;27:84–91
9. Suganami T, Yuan X, Shimoda Y, et al. Activating transcription factor 3 constitutes a negative feedback mechanism that attenuates saturated Fatty acid/toll-like receptor 4 signaling and macrophage activation in obese adipose tissue. Circ Res 2009;105:25–32
10. Matsumoto M, Tanaka T, Kaisho T, et al. A novel LPS-inducible C-type lectin is a transcriptional target of NF-IL6 in macrophages. J Immunol 1999;163:5039–5048
11. Poltorak A, He X, Smirnova I, et al. Defective LPS signaling in C3H/HeJ and C57BL/10ScCr mice: mutations in Tlr4 gene. Science 1998;282:2085–2088
12. Hironaka N, Mochida K, Mori N, Maeda M, Yamamoto N, Yamaoka S. Tax-independent constitutive IkappaB kinase activation in adult T-cell leukemia cells. Neoplasia 2004;6:266–278
13. Tomita S, Fujita T, Kirino Y, Suzuki T. PDZ domain-dependent suppression of NF-kappaB/p65-induced Abeta42 production by a neuron-specific X11-like protein. J Biol Chem 2000;275:13056–13060
14. Yamauchi A, Kim C, Li S, et al. Rac2-deficient murine macrophages have selective defects in superoxide production and phagocytosis of opsonized particles. J Immunol 2004;173:5971–5979
15. Ito A, Suganami T, Yamauchi A, et al. Role of CC chemokine receptor 2 in bone marrow cells in the recruitment of macrophages into obese adipose tissue. J Biol Chem 2008;283:35715–35723
16. Wells CA, Salvage-Jones JA, Li X, et al. The macrophage-inducible C-type lectin, mincle, is an essential component of the innate immune response to Candida albicans. J Immunol 2008;180:7404–7413
17. Schoenen H, Bodendorfer B, Hitchens K, et al. Cutting edge: Mincle is essential for recognition and adjuvanticity of the mycobacterial cord factor and its synthetic analog trehalose-dibehenate. J Immunol 2010;184:2756–2760
18. Yamasaki S, Matsumoto M, Takeuchi O, et al. C-type lectin Mincle is an activating receptor for pathogenic fungus, Malassezia. Proc Natl Acad Sci USA 2009;106:1897–1902
19. Ishikawa E, Ishikawa T, Morita YS, et al. Direct recognition of the mycobacterial glycolipid, trehalose dimycolate, by C-type lectin Mincle. J Exp Med 2009;206:2879–2888
20. Lee JY, Sohn KH, Rhee SH, Hwang D. Saturated fatty acids, but not unsaturated fatty acids, induce the expression of cyclooxygenase-2 mediated through Toll-like receptor 4. J Biol Chem 2001;276:16683–16689
21. Suganami T, Mieda T, Itoh M, Shimoda Y, Kamei Y, Ogawa Y. Attenuation of obesity-induced adipose tissue inflammation in C3H/HeJ mice carrying a Toll-like receptor 4 mutation. Biochem Biophys Res Commun 2007;354:45–49
22. Heilbronn LK, Campbell LV. Adipose tissue macrophages, low grade inflammation and insulin resistance in human obesity. Curr Pharm Des 2008;14:1225–1230
23. Zeyda M, Farmer D, Todoric J, et al. Human adipose tissue macrophages are of an anti-inflammatory phenotype but capable of excessive pro-inflammatory mediator production. Int J Obes (Lond) 2007;31:1420–1428
24. Zeyda M, Stulnig TM. Adipose tissue macrophages. Immunol Lett 2007;112:61–67
25. Gordon S, Taylor PR. Monocyte and macrophage heterogeneity. Nat Rev Immunol 2005;5:953–964
26. Medzhitov R. Origin and physiological roles of inflammation. Nature 2008;454:428–435
27. Tsukumo DM, Carvalho-Filho MA, Carvalheira JB, et al. Loss-of-function mutation in Toll-like receptor 4 prevents diet-induced obesity and insulin resistance. Diabetes 2007;56:1986–1998
28. Itoh M, Suganami T, Satoh N, et al. Increased adiponectin secretion by highly purified eicosapentaenoic acid in rodent models of obesity and human obese subjects. Arterioscler Thromb Vasc Biol 2007;27:1918–1925
29. Yamasaki S, Ishikawa E, Sakuma M, Hara H, Ogata K, Saito T. Mincle is an ITAM-coupled activating receptor that senses damaged cells. Nat Immunol 2008;9:1179–1188
30. Strissel KJ, Stancheva Z, Miyoshi H, et al. Adipocyte death, adipose tissue remodeling, and obesity complications. Diabetes 2007;56:2910–2918
31. Cinti S, Mitchell G, Barbatelli G, et al. Adipocyte death defines macrophage localization and function in adipose tissue of obese mice and humans. J Lipid Res 2005;46:2347–2355
32. Gringhuis SI, den Dunnen J, Litjens M, van Het Hof B, van Kooyk Y, Geijtenbeek TB. C-type lectin DC-SIGN modulates Toll-like receptor signaling via Raf-1 kinase-dependent acetylation of transcription factor NF-kappaB. Immunity 2007;26:605–616
33. Nakayama M, Underhill DM, Petersen TW, et al. Paired Ig-like receptors bind to bacteria and shape TLR-mediated cytokine production. J Immunol 2007;178:4250–4259

STEM CELLS AND DEVELOPMENT
Volume 20, Number 9, 2011

DOI: 10.1089/scd.2011.0074

Potential Therapeutic Application of Intravenous Autologous Bone Marrow Infusion in Patients with Alcoholic Liver Cirrhosis

Takafumi Saito,[1] Kazuo Okumoto,[1] Hiroaki Haga,[1] Yuko Nishise,[1] Rika Ishii,[1] Chikako Sato,[1] Hisayoshi Watanabe,[1] Akio Okada,[2] Motoki Ikeda,[2] Hitoshi Togashi,[3] Tsuyoshi Ishikawa,[4] Shuji Terai,[4] Isao Sakaida,[4] and Sumio Kawata[1]

The present study was conducted to evaluate the application and efficacy of autologous bone marrow infusion (ABMi) for improvement of liver function in patients with alcoholic liver cirrhosis (ALC). Five subjects and 5 control patients with ALC who had abstained from alcohol intake for 24 weeks before the study were enrolled. Autologous bone marrow cells were washed and injected intravenously, and the changes in serum liver function parameters, and the level of the type IV collagen 7S domain as a marker of fibrosis, were monitored for 24 weeks. The distribution of activated bone marrow was assessed by indium-111-chloride bone marrow scintigraphy. The number of cells infused was $8.0 \pm 7.3 \times 10^9$ (mean ± standard error). The serum levels of albumin and total protein and the prothrombin time were significantly higher during the follow-up period after ABMi than during the observation period in treated patients, whereas no such changes were observed in the controls. In the patients who received ABMi, the Child-Pugh score decreased in all 3 who were classified as class B; the serum levels of type IV collagen 7S domain improved in 4 of the 5 patients; and bone marrow scintigraphy demonstrated an increase of indium-111-chloride uptake in 3 of the 4 patients tested. ABMi for patients with ALC helps improve liver function parameters in comparison with observation during abstinence and ameliorates the degree of fibrosis in terms of serum markers and bone marrow activation in most cases.

Introduction

LIVER CIRRHOSIS IS THE END stage of chronic liver disease, and it is associated with many serious systemic complications resulting from both liver failure and portal hypertension. This condition has a poor prognosis and is difficult to treat. Liver transplantation is the only curative remedy, but it is associated with many problems such as donor shortage, surgical complications, rejection, and high cost. As an alternative approach, regenerative cell therapy using stem cells is now being investigated. In particular, multipotent stem cells present in bone marrow (BM) are a promising candidate for this purpose, and clinical trials aiming at therapy of cardiovascular diseases have been performed [1,2].

BM cells have been shown to be capable of differentiating into the liver cell lineage, and transplantation of BM cells has considerable potential for regeneration of liver tissue [3–6]. The degree of liver function and fibrosis as well as survival rate have been shown to improve significantly as a result of BM cell transplantation in animal models of severe liver injury [7,8]. We have experimentally investigated the potential of BM stem cells to differentiate into the hepatocyte lineage both in vitro or in vivo with a view to possible application for clinical trials aimed at liver regeneration [9–12]. In this context, the effectiveness of CD34+ hematopoietic stem cell injection into the liver via the portal vein or hepatic artery had been shown to improve the serum levels of albumin and bilirubin [13,14]. Our research group has already reported the therapeutic effectiveness of whole-BM peripheral infusion, referred to as autologous BM cell infusion (ABMi) therapy for patients with cirrhosis with hepatitis B or C [15,16].

Alcoholic liver injury is a common liver disease worldwide. Although disease activity may be decreased by abstinence in the initial phase, it eventually progresses to cirrhosis and finally to death unless patients receive appropriate therapeutic intervention for both liver injury and alcohol abuse. Even if patients discontinue alcohol intake, those in whom the disease has progressed to advanced cirrhosis with marked liver fibrosis have a poor prognosis because of

Departments of [1]Gastroenterology and [2]Radiology, Yamagata University School of Medicine, Yamagata, Japan.
[3]Health Administrative Center, Yamagata University, Yamagata, Japan.
[4]Department of Gastroenterology and Hepatology, Yamaguchi University Graduate School of Medicine, Ube, Yamaguchi, Japan.

serious complications and liver cell dysfunction. Therefore, such patients require some form of liver-regenerative therapy, as well as abstinence, to improve the liver function. Since such patients are free of pathogens such as hepatitis B or hepatitis C that cause continuous liver necroinflammation, ABMi might facilitate a degree of liver regeneration if abstinence is maintained along with appropriate nutritional care. Pai et al. reported that autologous infusion of expanded mobilized BM-derived CD34+ cells into patients with alcoholic liver cirrhosis (ALC) via the hepatic artery improved the serum levels of both bilirubin and transaminase, as well as the Child-Pugh score [17].

To investigate the effectiveness of ABMi for patients with ALC, we applied it to such patients and examined the resulting changes in liver function parameters. In addition, using indium-111-chloride (^{111}In) BM scintigraphy, we tracked the infused BM cells after ABMi.

Patients and Methods

Patients

Patients with a diagnosis of advanced liver cirrhosis due to alcoholic liver injury were enrolled. All the patients were negative for both anti-hepatitis C virus antibody and hepatitis B surface antigen and had a history of excessive alcohol consumption exceeding 60 g/day of ethanol for >5 years. The patients were interviewed, and those who had abstained for >24 weeks before the interview were entered into the study. The inclusion criteria for clinical parameters were as follows: platelet count >50,000/mm^3, total bilirubin <3 mg/dL, and absence of liver cancer on computed tomography (CT). Both heart and lung function were screened to confirm whether general anesthesia was possible. As a control group, we used patients who were not given ABMi, but who agreed to the use of their clinical data for study. Those patients had also been diagnosed as having ALC, and were matched to the subjects who received ABMi for age, sex, medication, and various biochemical parameters; their liver function parameters were compared with those of the subjects who received ABMi during the study period.

Autologous BM cell preparation and infusion into patients

A total of 400 mL BM was harvested from the ilium according to the standard procedure under general anesthesia and collected in a plastic bag containing heparin. After fat had been removed from the top of the bag, hydroxyethyl starch was added to a final concentration of 1%. Red blood cells were precipitated after 40 min of incubation at room temperature. We used an automated bench-top device (Cytomate; Takara Bio Inc., Otsu, Shiga, Japan), which is a functionally closed system incorporating a spinning membrane connected to a filter wash bag, for washing and concentrating the mononuclear cells (MNCs). The final cell products were washed, concentrated, and made up to a final volume of 105 mL. Five milliliters of the final cell product was subjected to the trypan blue dye exclusion test, endotoxin test, and fluorescence-activated cell sorting analysis. CD34+, CD44+, CD45+, and CD117+ cells were determined by flow cytometry at the central laboratory of SRL Inc., Tokyo, Japan. At 6 h after BM harvest, the final MNCs preparation was administered to each patient via the cubital vein by drip infusion. All the study protocols were approved by the ethics committee of Yamagata University School of Medicine, and written informed consent was obtained from all participants.

Follow-up of serological tests for liver function and fibrosis

The patients were followed up, and laboratory data were analyzed for 48 weeks in total, which included analyses once a month for 24 weeks before and after ABMi therapy. Patients who consumed more than 20 g alcohol/day during the analysis period were considered to have dropped out and excluded from further analysis. Primary outcomes were the safety and feasibility of ABMi therapy for ALC. The serum parameters representing liver function, including serum albumin, total protein, and prothrombin time, were evaluated before and after ABMi therapy. The Child-Pugh score calculated by summing the total points for the serum levels of albumin and total bilirubin, prothrombin time, ascites, and encephalopathy was used to evaluate the overall condition of patients with cirrhosis. To evaluate the changes in the degree of liver fibrosis in patients receiving ABMi, the serum levels of the type IV collagen 7S domain was monitored during the follow-up period. The liver function parameters of the control patients who succeeded in maintaining abstinence were followed up for the same period as that of patients who received ABMi.

Liver function calculated by single photon emission CT analysis

Analysis of the liver using single photon emission CT (SPECT) with a radiolabeled, specific hepatic binding protein, technetium 99m galactosyl-human serum albumin (Tc-GSA), was carried out according to the procedure we have previously reported [18]. SPECT analysis is useful for assessment of hepatic functional reserve [19,20]. Briefly, Tc-GSA (185 MBq) was injected intravenously, and SPECT data were obtained from 12 min 30 s to 17 min 30 s after the injection using a triple-headed camera (MULTISPECT 3; Siemens Medical Systems, Erlangen, Germany). The liver uptake ratio, that is, the actual percentage of the administered Tc-GSA dose incorporated into the liver, was quantified by calculating the percentage of the hepatic SPECT value relative to the preinjection syringe value. The liver volume was obtained from the SPECT data and calculated by the outline extraction method to determine the functional liver volume in cm^3. The liver uptake ratio was then divided by the functional liver volume to obtain the liver uptake ratio per unit volume (liver uptake density; %/cm^3). We assessed the obtained liver uptake density values of patients receiving ABMi before the treatment and 2 weeks after.

BM imaging by ^{111}In scintigraphy

BM scintigraphy using ^{111}In was performed in 4 of the 5 patients before and 1 week after ABMi therapy. BM scintigraphy is useful for evaluating the distribution of activated BM, mainly hematopoietic stem cells. The scintigraphy was conducted 48 h after an intravenous injection of ^{111}In (74 MBq). The total ^{111}In count was divided by the total number of pixels on the computer screen to obtain the ^{111}In

count per pixel, and this was used as an index of BM activation in patients before and 1 week after ABMi.

Statistical analysis

Statistical analysis was performed using *t*-test for paired or unpaired samples. Time courses of measurements of liver function parameters were analyzed by repeated-measures ANOVA. A 2-tailed P value of <0.05 was considered statistically significant. The data were expressed as mean ± standard error. Analyses were performed using SPSS version 15.0 for Windows (SRSS, Chicago, IL).

Results

Patients characteristics

Five patients received ABMi therapy and were followed up. The baseline demographic features and clinical characteristics of these 5 patients are shown in Table 1. All the patients were men with a mean age of 64 (range: 59–75) years. One patient had ascites, and the other 4 had a history of ascites. All patients had previously undergone endoscopic sclerosing therapy for esophageal varices. CT demonstrated macroscopic cirrhosis with a high degree of liver deformity, and all patients had undergone liver biopsy before the study, which confirmed cirrhosis histologically. The baseline data for the patients who received ABMi in comparison with those for the controls with alcoholic cirrhosis who were matched for age, sex, medication, and liver function parameters are shown in Table 2. There were no significant differences in these baseline data between the 2 groups.

Cell products for ABMi and their characteristics

The characteristics of the cell products for ABMi are shown in Table 3. From 400 mL of autologous BM harvested from the ilium of each patient, the mean number of infused MNCs was $8.0 \pm 7.3 \times 10^9$. The viability of the MNCs was >90% in all cases. The percentages of CD34+, CD44+, CD45+, and CD117+ cells were 6.0% ± 1.8%, 90.1% ± 5.6%, 81.2% ± 6.4%, and 12.0% ± 3.5%, respectively.

Changes in biochemical parameters before and after ABMi

The 5 patients receiving ABMi therapy were followed up for 48 weeks in total: for 24 weeks before and for 24 weeks after ABMi. The 5 controls were also followed up for a total of 48 weeks. Medication was not changed during the study period in any of the patients. The changes of liver function parameters, including serum albumin, total protein, and prothrombin time, are shown in Fig. 1. These parameters all showed an improvement in the patients who received ABMi; the mean level of serum albumin before and 24 weeks after ABMi improved from 3.3 ± 0.2 to 3.8 ± 0.2 g/dL, that of total protein improved from 6.9 ± 0.2 to 7.7 ± 0.1 g/dL, and the prothrombin time improved from 76.6% ± 6.1% to 87.6 % ± 6.0%. The levels of serum albumin, total protein, and prothrombin time during the follow-up period after ABMi were significantly higher than those during the period before ABMi (serum albumin; $P=0.02$, total protein; $P=0.03$, prothrombin time; $P<0.01$). However, no significant changes were observed in the levels of serum albumin and total protein, or prothrombin time, in the controls during the 48 weeks of observation. The Child-Pugh score decreased from 6.8 ± 1.3 before ABMi to 5.8 ± 0.8 at 24 weeks after ABMi. All of the 3 patients who were classified as Child class B with 7 points or higher before ABMi showed a decrease in their scores after ABMi therapy, and the remaining 2 patients classified as Child class A with 6 points or lower showed no change in their scores (Fig. 2).

Changes in liver fibrosis markers

The serum level of the type IV collagen 7S domain was evaluated in patients before and 24 weeks after ABMi. Improvement was observed in 4 of the 5 cases except for case no.5 at 24 weeks after ABMi therapy. The serum levels of the type IV collagen 7S domain decreased from 10.0 ± 3.9 ng/mL before to 8.1 ± 2.3 at 24 weeks after ABMi (Fig. 3), although the change was not significant ($P=0.33$), given the small number of cases examined.

Estimation of liver function using Tc-GSA SPECT

The functional index was improved at 2 weeks in 4 of the 5 patients who received ABMi therapy, and was unchanged in one (case no.1). The mean functional index calculated by Tc-GSA SPECT tended to increase from $2.4 \pm 0.5 \times 10^{-2}$ before ABMi to $2.7 \pm 0.6 \times 10^{-2}$ at 2 weeks after ($P=0.09$) (Fig. 4).

TABLE 1. PATIENT CHARACTERISTICS

							Serum markers					
	Age	*Sex*	*Etiology*	*Ascites*	*Coma*	*Varices*	*T.protein (g/dL)*	*Albumin (g/dL)*	*T.bilirubin (mg/dL)*	*PT (%)*	*ICG R15 (%)(K-ICG)*	*C-P score*
Patient 1	59	M	Alcohol	None (1)[a]	None (1)	positive[b]	6.5	2.7 (3)	1.0 (1)	67 (2)	40 (0.060)	8
Patient 2	61	M	Alcohol	None (1)[a]	None (1)	positive[b]	6.4	2.9 (2)	1.3 (1)	67 (2)	33 (0.077)	7
Patient 3	60	M	Alcohol	None (1)[a]	None (1)	positive[b]	6.7	3.8 (1)	0.8 (1)	92 (1)	27 (0.107)	5
Patient 4	75	M	Alcohol	None (1)[a]	None (1)	positive[b]	7.3	3.3 (2)	2.0 (2)	66 (2)	67 (0.043)	8
Patient 5	69	M	Alcohol	Minimal (2)	None (1)	positive[b]	7.7	3.7 (1)	1.5 (1)	91 (1)	46 (0.073)	6

Number in parentheses indicates points in total Child-Pugh (C-P) score.
[a]History of ascites.
[b]History of endoscopic sclerosing therapy.
T.protein, total protein; T.bilirubin, total bilirubin; PT, prothrombin time activity; ICG-R15, indocyanin green test, retention 15 min.

TABLE 2. BASELINE DATA OF AUTOLOGOUS BONE MARROW INFUSION GROUP AND CONTROL GROUP

Variable	ABMi group (n=5)	Control group (n=5)	P
Sex (male)	5	5	
Age (years)	64.6±2.9	61.2±4.5	N.S.
Total protein (g/dL)	6.92±0.25	7.22±0.38	N.S.
Serum albumin (g/dL)	3.28±0.22	3.28±0.06	N.S.
Total bilirubin (mg/dL)	1.36±0.20	1.38±0.25	N.S.
Prothrombin time (%)	76.6±6.1	84.8±7.2	N.S.
Medication			
Diuretics	3	3	
BCAA products	4	5	

N.S., not significant (*t*-test). The data are expressed by mean±standard error.

BCAA, branched chain amino acids; ABMi, autologous bone marrow infusion.

Activated BM distribution assessed by ^{111}In scintigraphy

The ^{111}In count per pixel was increased in 3 of the 4 patients tested at 1 week after ABMi therapy, but was not increased in case no.5. The average ^{111}In count per pixel in these 4 cases increased from 3.7±0.9 before ABMi to 4.4±1.3 at 1 week after (Fig. 5A), although the changes were not significant ($P=0.23$), given the small number of cases. The BM image in case no. 2, with the highest increase in the ^{111}In count after ABMi therapy, is shown in Fig. 5B. Activation of BM cells in case no.2 was demonstrated by an increase in the ^{111}In count per pixel from 4.5 before to 6.3 at 1 week after ABMi.

Complications

None of the 5 patients who received ABMi therapy exhibited any serious complications during or after the procedure.

Discussion

This study showed that ABMi for patients with ALC could be performed safely under general anesthesia and that it improved their liver function parameters including the serum levels of albumin and total protein and the prothrombin time. The Child-Pugh score also improved in all 3 patients who had a score higher than 7, which was classified as class B. Further, ABMi resulted in induction of hepatic functional reserve, as suggested by Tc-GSA SPECT imaging as well as reduction of the serum levels of the fibrosis marker in 4 of the 5 cases examined.

It is generally accepted that the results of laboratory tests can be modified by drug administration or infusion of albumin products or plasma. Although both patients treated with ABMi and controls had received several types of medication, the administered drugs were not changed during the study period, whereas the patients abstained from alcohol and no blood products were supplied. Abstinence is an important factor to consider when selecting patients for ABMi, because ALC is an irreversible liver condition resulting from chronic inflammation attributable to the toxic effect of ethanol on the liver. For enrollment in the present study, patients who showed marked deformity of the liver on CT, and histologically proved cirrhosis, were required to have abstained from alcohol for at least 24 weeks. No changes in liver function parameters were found as a result of an abstinence in either the controls or the patients treated with ABMi in the period before ABMi. However, the results of the present study suggest that liver function parameters can be improved by ABMi in patients with ALC. A recent study has shown that patients who undergo orthotropic liver transplantation for alcoholic liver disease have a rate of recidivism as high as 28% at 9 years [21]. Therefore, both careful observation and adequate intervention in relation to abstinence may be required for patients after ABMi.

Although BM stem cell treatment for liver cirrhosis is an attractive strategy in the field of liver regenerative cell therapy, many concerns need to be addressed [22,23]. It is still unclear how infused BM cells work for the improvement of liver function. We have demonstrated experimentally that BM cells transplanted into the spleen of rats with liver damage induced by carbon tetrachloride express liver-specific proteins such as alpha-fetoprotein in their cytoplasm in the recipient liver [10]. A clinical trial of ABMi for patients with cirrhosis has also demonstrated that the number of alpha-fetoprotein-positive cells was increased significantly in the liver, relative to the situation before ABMi. In addition, ABMi appeared to induce hepatocyte proliferation in the liver, as expression of proliferating cell nuclear antigen, a marker of hepatocyte proliferation, was significantly increased after ABMi in comparison with the pretreatment situation [15]. Another study has shown that intraportal administration of autologous CD133+ BM cells and subsequent portal venous embolization of right liver segments resulted in a 2.5-fold increase in the mean proliferation rate of the left lateral segment, in comparison with controls not

TABLE 3. CHARACTERISTICS OF PROCESSED MONONUCLEAR CELLS

	Harvest vol. (mL)	No. of infused MNCs (X 10^9)	CD34+ (%)	CD44+ (%)	CD45+ (%)	CD117+ (%)
Patient 1	400	3.0	4.3	87.7	85.2	10.9
Patient 2	400	2.5	8.8	84.4	78.8	15.9
Patient 3	400	16.0	5.2	93.7	82.4	8.2
Patient 4	400	2.3	5.2	97.9	88.0	15.5
Patient 5	400	16.0	6.7	86.6	71.4	9.6
Mean±SE		8.0±7.3	6.0±1.8	90.1±5.6	81.2±6.4	12.0±3.5

MNC, mononuclear cell.

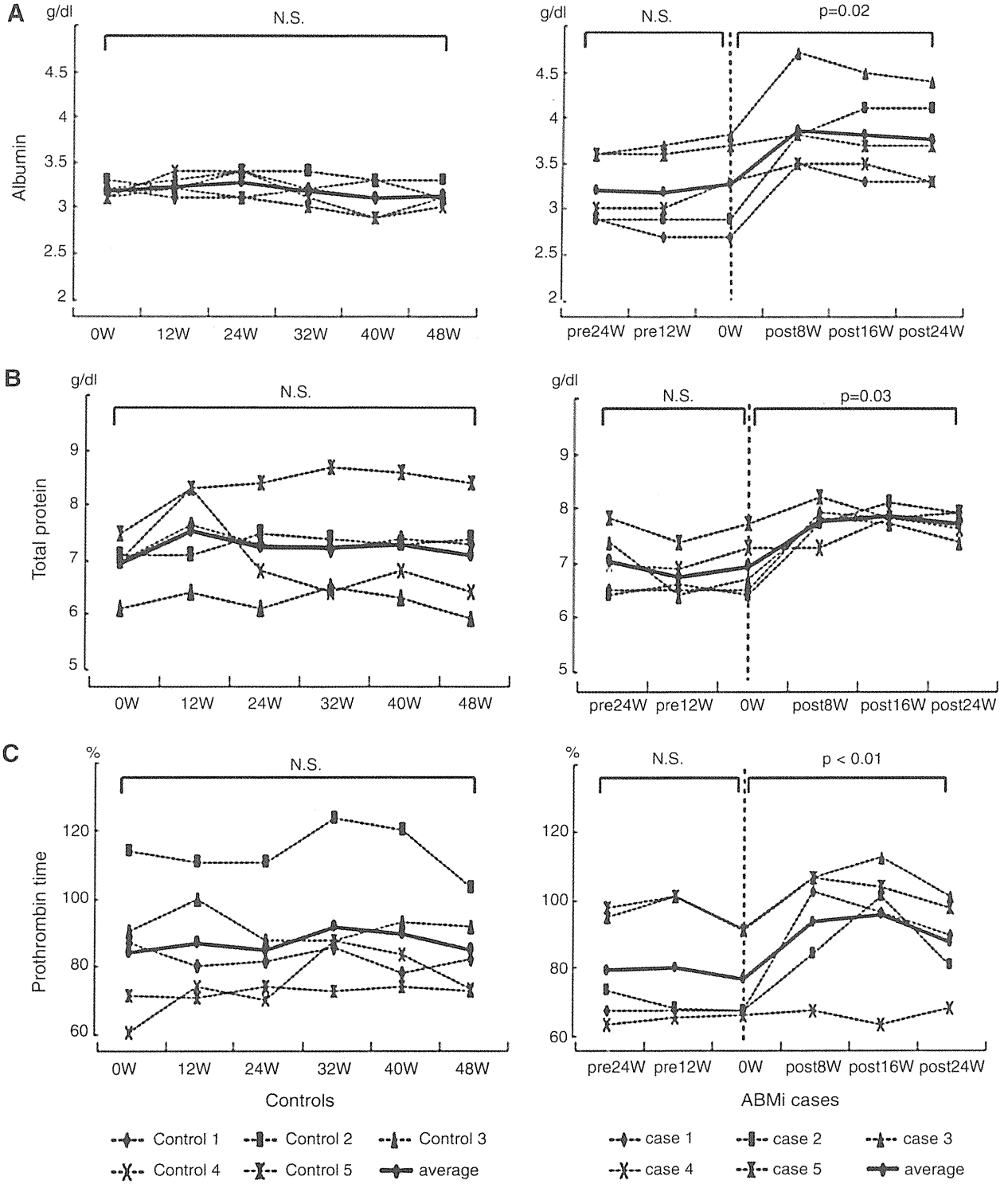

FIG. 1. Changes in biochemical parameters before and after ABMi. The levels of serum albumin **(A)** and total protein **(B)**, and prothrombin time **(C)**, during the follow-up of patients after ABMi were significantly higher than those during the period before ABMi. No significant changes were observed in the controls. ABMi, autologous bone marrow infusion.

receiving BM transfusion [24]. These data suggest that transplanted BM cells have a potential role in liver regeneration and proliferate in the recipient liver and that this process is likely to occur early after ABMi, as Tc-GSA SPECT analysis in the present study demonstrated an increase in the liver function index of most patients 2 weeks after ABMi. However, since it is still unclear whether fully functional hepatocytes are induced by ABMi, the characteristics of BM

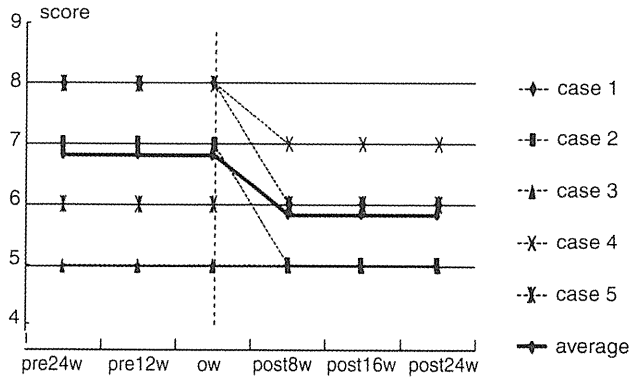

FIG. 2. Changes in Child-Pugh score after ABMi in comparison with those before. The Child-Pugh score decreased from 6.8±1.3 before ABMi to 5.8±0.8 at 24 weeks after ABMi. All of the 3 patients classified as class B, scoring 7 points or higher before ABMi, showed a decrease in their scores after the therapy.

stem cells that show hepatocyte differentiation should be elucidated further. In addition, to elucidate the cell-cell communication in the extracellular microenvironment that would be important for tissue repair, many markers originating from the different cell types among MNCs should be investigated in the future.

The tracking of BM cells infused into the human body as a means of monitoring cell engraftment after ABMi has not been previously reported. In the present study, BM scintigraphy using ^{111}In before and after ABMi showed that the distribution of activated BM was enhanced systemically after ABMi, including the liver, in 3 of the 4 patients examined. Although the process of migration of infused BM cells to the

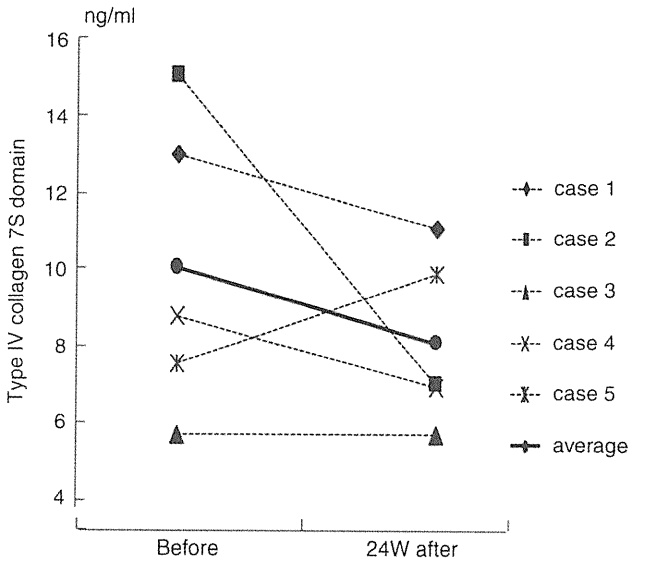

FIG. 3. Changes in the levels of a liver fibrosis marker after ABMi in comparison with those before. The level of the type IV collagen 7S domain improved in 4 of the 5 cases, with the exception of case no.5, at 24 weeks after ABMi therapy, and their serum levels decreased from 10.0±3.9 ng/mL before to 8.1±2.3 ng/mL at 24 weeks after the therapy.

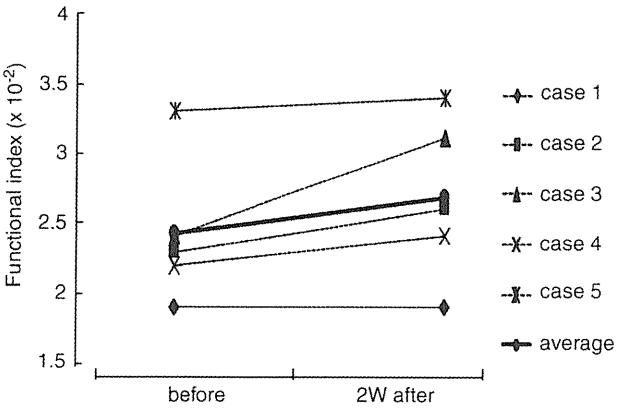

FIG. 4. Estimation of liver function using technetium 99m galactosyl-human serum albumin single photon emission computed tomography. The functional index improved in 4 of the 5 cases, and did not change in one (case 1) after ABMi. The mean functional index tended to increase from $2.4\pm0.5\times10^{-2}$ before ABMi to $2.7\pm0.6\times10^{-2}$ at 2 weeks after ($P=0.09$).

liver remains unknown, clarification of the factors responsible could yield important data for improving the efficiency of transplantation. In fact, ABMi case no. 2, in which the greatest increase in the ^{111}In count was observed 1 week after ABMi, showed a marked decrease in the concentration of the

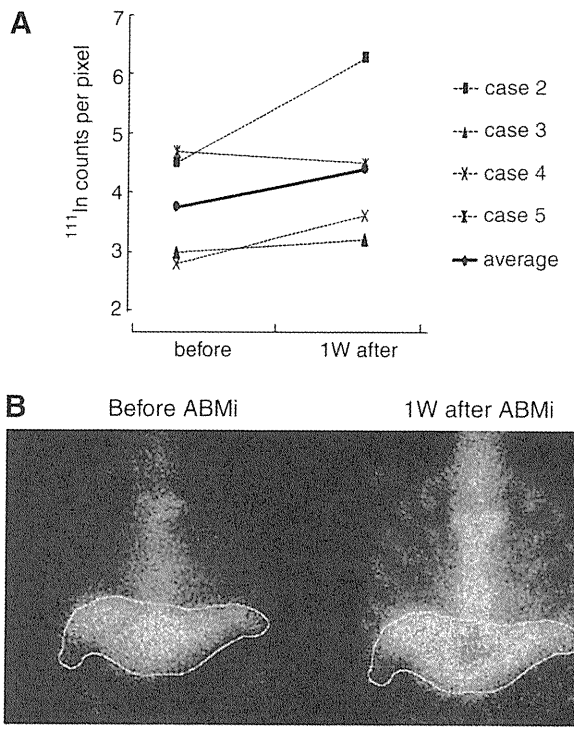

FIG. 5. Activated BM distribution demonstrated by indium-111-chloride (^{111}In) scintigraphy. **(A)** The ^{111}In count per pixel increased in 3 of the 4 patients tested after ABMi therapy, with the exception of case no.5. The average ^{111}In count per pixel in the 4 patients increased from 3.7±0.9 before to 4.4±1.3 after ABMi. **(B)** BM image of case no. 2, showing the greatest increase of the ^{111}In count 1 week after ABMi therapy (4.5 before to 6.3 after).

type IV collagen 7S domain, as shown in Fig. 3, as well as a marked improvement of liver function parameters, as shown in Fig. 1. In contrast, ABMi case no.5 was only one showing no change in the ^{111}In count at 1 week after ABMi, and the only case in which the level of the type IV collagen 7S domain did not decrease after ABMi. Effective migration of infused BM cells to the liver may ameliorate liver fibrosis, because such cells have been shown experimentally to produce and secrete anti-fibrosis factors such as matrix metalloproteinase-9 [7]. At this time, the factors that determine the difference between effectiveness and noneffectiveness are unclear. Collateral circulation resulting from the portal vein disorganization that characterizes liver cirrhosis may affect the flow and effective migration of infused BM cells to the liver, and, thus, migration of infused cells to the liver may partly depend on the portal venous pressure. Further, the expression levels of cellular adhesion molecules associated with the attachment of infused cells to liver tissue may vary a great deal among patients. It is important to determine the adhesion molecules that are induced in the liver tissue of patients receiving ABMi. Further studies are needed to clarify the mechanisms involved in the migration of infused BM cells to the liver.

The present study did not demonstrate the long-term effectiveness of this therapy in terms of survival rate or improvement in the quality of life. Such effects will need to be evaluated by a randomized controlled study in the future. In addition, improvements in the methods of delivering infused BM cells to the human body should also be investigated further. We are currently conducting experiments aimed at improving the effectiveness of this therapy by investigating the long-term culture conditions for BM cells, the optimum cell population to be employed, the effectiveness of repeated transplantation of BMCs, and the optimum route of cell delivery. We have already confirmed both the safety and short-term efficacy of ABMi therapy for various liver diseases [15,16], and these basic data are expected to be of value for improving ABMi therapy in the near future.

In summary, ABMi therapy for patients with alcoholic cirrhosis has been shown to improve liver function parameters, in contrast to observation accompanied by abstinence from alcohol. The markers of liver fibrosis, hepatic functional reserve, and BM cell activation were improved in most of the patients who received ABMi therapy. However, the degree of effectiveness of ABMi is likely to differ among patients, and the present results should still be considered in terms of a pilot study. Further investigation of factors associated with the effectiveness of this therapy is warranted, and future studies will need to assess the safety of this therapy and its effect on liver function in a large number of patients, together with its long-term effectiveness, in terms of survival rate and quality of life.

Acknowledgments

This study was supported in part by a grant from the Ministry of Health, Labor, and Welfare of Japan, and also in part by a Grant-in-Aid from the Global COE program of the Japan Society for the Promotion of Science. The authors thank Dr. K. Okita for his support toward this study.

Author Disclosure Statement

The authors declare that they have no conflict of interest.

References

1. Krause K, C Schneider, KH Kuck and K Jaquet. (2010). Stem cell therapy in cardiovascular disorders. Cardiovasc Ther 28:e101–e110.
2. Bui QT, ZM Gertz and RL Wilensky. (2010). Intracoronary delivery of bone-marrow-derived stem cells. Stem Cell Res Ther 1:29.
3. Petersen BE, WC Bowen, KD Patrene, WM Mars, AK Sullivan, N Murase, SS Boggs, JS Greenberger and JP Goff. (1999). Bone marrow as a potential source of hepatic oval cells. Science 284:1168–1170.
4. Alison MR, R Poulsom, R Jeffery, AP Dhillon, A Quaglia, J Jacob, M Novelli, G Prentice, J Williamson and NA Wright. (2000). Hepatocytes from non-hepatic adult stem cells. Nature 406:257.
5. Theise ND, S Badve, R Saxena, O Henegariu, S Sell, JM Crawford and DS Krause. (2000). Derivation of hepatocytes from bone marrow cells in mice after radiation-induced myeloablation. Hepatology 31:235–240.
6. Theise ND, M Nimmakayalu, R Gardner, PB Illei, G Morgan, L Teperman, O Henegariu and DS Krause. (2000). Liver from bone marrow in humans. Hepatology 32:11–16.
7. Sakaida I, S Terai, N Yamamoto, K Aoyama, T Ishikawa, H Nishina and K Okita. (2004). Transplantation of bone marrow cells reduces CCl4-induced liver fibrosis in mice. Hepatology 40:1304–1311.
8. Terai S, I Sakaida, N Yamamoto, K Omori, T Watanabe, S Ohata, T Katada, K Miyamoto, K Shinoda, H Nishina and K Okita. (2003). An in vivo model for monitoring transdifferentiation of bone marrow cells into functional hepatocytes. J Biochem 134:551–558.
9. Okumoto K, T Saito, E Hattori, JI Ito, A Suzuki, K Misawa, R Ishii, T Karasawa, H Haga, M Sanjo, T Takeda, K Sugahara, K Saito, H Togashi and S Kawata. (2005). Differentiation of rat bone marrow cells cultured on artificial basement membrane containing extracellular matrix into a liver cell lineage. J Hepatol 43:110–116.
10. Okumoto K, T Saito, E Hattori, JI Ito, A Suzuki, K Misawa, M Sanjyo, T Takeda, K Sugahara, K Saito, H Togashi and S Kawata. (2005). Expression of Notch signaling markers in bone marrow cells that differentiate into a liver cell lineage in a rat transplanted model. Hepatol Res 31:7–12.
11. Okumoto K, T Saito, H Haga, E Hattori, R Ishii, T Karasawa, A Suzuki, K Misawa, M Sanjo, JI Ito, K Sugahara, K Saito, H Togashi and S Kawata. (2006). Characteristics of rat bone marrow cells differentiated into a liver cell lineage and dynamics of the transplanted cells in the injured liver. J Gastroenterol 41:62–69.
12. Haga H, T Saito, K Okumoto, S Ugajin, C Sato, R Ishii, Y Nishise, J Ito, H Watanabe, K Saito, H Togashi and S Kawata. (2011). Enhanced expression of fibroblast growth factor 2 in bone marrow cells and its potential role in the differentiation of hepatic epithelial stem-like cells into hepatocyte lineage. Cell Tissue Res 343:371–378.
13. Gordon MY, N Levicar, M Pai, P Bachellier, I Dimarakis, F Al-Allaf, H M'Hamdi, T Thalji, JP Welsh, SB Marley, J Davies, F Dazzi, F Marelli-Berg, P Tait, R Playford, L Jiao, S Jensen, JP Nicholls, A Ayav, M Nohandani, F Farzaneh, J Gaken, R Dodge, M Alison, JF Apperley, R Lechler and NA Habib. (2006). Characterization and clinical application of human CD34+ stem/progenitor cell populations mobilized into the blood by granulocyte colony-stimulating factor. Stem Cells 24:1822–1830.

14. Levicar N, M Pai, NA Habib, P Tait, LR Jiao, SB Marley, J Davis, F Dazzi, C Smadja, SL Jensen, JP Nicholls, JF Apperley and MY Gordon. (2008). Long-term clinical results of autologous infusion of mobilized adult bone marrow derived CD34+ cells in patients with chronic liver disease. Cell Prolif 41 (Suppl 1):115–125.
15. Terai S, T Ishikawa, K Omori, K Aoyama, Y Marumoto, Y Urata, Y Yokoyama, K Uchida, T Yamasaki, Y Fujii, K Okita and I Sakaida. (2006). Improved liver function in patients with liver cirrhosis after autologous bone marrow cell infusion therapy. Stem Cells 24:2292–2298.
16. Kim JK, YN Park, JS Kim, MS Park, YH Paik, JY Seok, YE Chung, HO Kim, KS Kim, SH Ahn, DY Kim, MJ Kim, KS Lee, CY Chon, SJ Kim, S Terai, I Sakaida and KH Han. (2010). Autologous bone marrow infusion activates the progenitor cell compartment in patients with advanced liver cirrhosis. Cell Transplant 19:1237–1246.
17. Pai M, D Zacharoulis, MN Milicevic, S Helmy, LR Jiao, N Levicar, P Tait, M Scott, SB Marley, K Jestice, M Glibetic, D Bansi, SA Khan, D Kyriakou, C Rountas, A Thillainayagam, JP Nicholls, S Jensen, JF Apperley, MY Gordon and NA Habib. (2008). Autologous infusion of expanded mobilized adult bone marrow-derived CD34+ cells into patients with alcoholic liver cirrhosis. Am J Gastroenterol 103:1952–1958.
18. Sugahara K, H Togashi, K Takahashi, Y Onodera, M Sanjo, K Misawa, A Suzuki, T Adachi, J Ito, K Okumoto, E Hattori, T Takeda, H Watanabe, K Saito, T Saito, Y Sugai and S Kawata. (2003). Separate analysis of asialoglycoprotein receptors in the right and left hepatic lobes using Tc-GSA SPECT. Hepatology 38:1401–1409.
19. Kudo M, A Todo, K Ikekubo, K Yamamoto, DR Vera and RC Stadalnik. (1993). Quantitative assessment of hepatocellular function through in vivo radioreceptor imaging with technetium 99m galactosyl human serum albumin. Hepatology 17:814–819.
20. Kwon AH, SK Ha-Kawa, S Uetsuji, Y Kamiyama and Y Tanaka. (1995). Use of technetium 99m diethylenetriaminepentaacetic acid-galactosyl-human serum albumin liver scintigraphy in the evaluation of preoperative and postoperative hepatic functional reserve for hepatectomy. Surgery 117:429–434.
21. Biselli M, A Gramenzi, M Del Gaudio, M Ravaioli, G Vitale, S Gitto, GL Grazi, AD Pinna, P Andreone and M Bernardi; Bologna Liver Transplantation Group. (2010). Long term follow-up and outcome of liver transplantation for alcoholic liver disease: a single center case-control study. Clin Gastroenterol 44:52–57.
22. Kallis YN, MR Alison and SJ Forbes. (2007). Bone marrow stem cells and liver disease. Gut 56:716–724.
23. Lorenzini S and P Andreone. (2007). Stem cell therapy for human liver cirrhosis: a cautious analysis of the results. Stem Cells 25:2383–2384.
24. am Esch JS 2nd, WT Knoefel, M Klein, A Ghodsizad, G Fuerst, LW Poll, C Piechaczek, ER Burchardt, N Feifel, V Stoldt, M Stockschläder, N Stoecklein, RY Tustas, CF Eisenberger, M Peiper, D Häussinger and SB Hosch. (2005). Portal application of autologous CD133+ bone marrow cells to the liver: a novel concept to support hepatic regeneration. Stem Cells 23:463–470.

Address correspondence to:
Dr. Takafumi Saito
Department of Gastroenterology
Yamagata University School of Medicine
2-2-2 Iida-nishi
Yamagata 990-9585
Japan

E-mail: tasaitoh@med.id.yamagata-u.ac.jp

Received for publication February 16, 2011
Accepted after revision March 20, 2011
Prepublished on Liebert Instant Online March 20, 2011

Cell Tissue Res (2011) 343:371–378
DOI 10.1007/s00441-010-1093-2

REGULAR ARTICLE

Enhanced expression of fibroblast growth factor 2 in bone marrow cells and its potential role in the differentiation of hepatic epithelial stem-like cells into the hepatocyte lineage

Hiroaki Haga · Takafumi Saito · Kazuo Okumoto · Satoshi Ugajin · Chikako Sato · Rika Ishii · Yuko Nishise · Junitsu Ito · Hisayoshi Watanabe · Koji Saito · Hitoshi Togashi · Sumio Kawata

Received: 4 August 2010 / Accepted: 17 November 2010 / Published online: 9 December 2010

Abstract The transplantation of bone marrow cells (BMCs) has been applied in liver regenerative cell therapy. However, details of the interaction between the transplanted BMCs and hepatic stem cells have not been elucidated. The aim of the present study was to investigate the interaction of BMCs with hepatic stem-like cells (HSLCs) and to determine the BMC factor that steers HSLC differentiation into the hepatocyte lineage. Both BMCs and HSLCs were obtained from an adult Sprague-Dawley rat, and a co-culture system was established. Cell proliferation was analyzed by a proliferation assay, and the differentiation of HSLCs into the hepatocyte lineage was evaluated by the detection of cellular mRNA for liver-specific proteins. DNA microarray analysis was applied to BMCs co-cultured with HSLCs to determine the genes upregulated by their interaction. The proliferation of HSLCs co-cultured with BMCs was significantly higher than that of HSLCs cultured alone, and the expression of mRNAs for both *albumin* and *tryptophan-2,3-dioxygenase* was detectable in the co-cultured HSLCs. DNA microarray analysis showed the upregulated expression of *fibroblast growth factor 2* (*FGF2*) mRNA in BMCs co-cultured with HSLCs, and the expression of mRNAs for both *albumin* and *tyrosine aminotransferase* became detectable in HSLCs cultured with FGF2. Thus, BMCs stimulate both the proliferation of HSLCs and their differentiation into the hepatocyte lineage. FGF2 is one of the factors that is produced by the interacting BMCs and that stimulates this differentiation.

Keywords Bone marrow · Hepatic stem cell · Interaction · FGF2 · Differentiation · Rat (Sprague-Dawley)

Introduction

Bone marrow cells (BMCs) have been shown to have the ability to differentiate into the liver cell lineage (Petersen et al. 1999; Alison et al. 2000; Theise et al. 2000a, b). Petersen et al. (1999) were the first to demonstrate that a population of rat BM stem cells is able to differentiate into hepatocytes and bile duct cells. We have previously reported that rat BMCs cultured on an artificial basement membrane containing extracellular matrix (ECM) with hepatocyte growth factor (HGF) have an enhanced tendency to differentiate into the liver cell lineage and proliferate (Okumoto et al. 2005a). Furthermore, in vivo experiments have revealed that transplanted rat BMCs become localized in the portal areas of the recipient's liver and express liver-cell-specific proteins (Theise et al. 2000a; Okumoto et al. 2005b). Recently, autologous BMC transplantation (a technique known as autologous BMC infusion therapy) has been applied to patients with liver cirrhosis and noted to improve the serum levels of albumin and total protein

This study was supported in part by a Grant-in-Aid from the Global COE program of the Japanese Society for the Promotion of Science and also in part by a grant from the Ministry of Health, Labor, and Welfare of Japan.

H. Haga · T. Saito (✉) · K. Okumoto · S. Ugajin · C. Sato · R. Ishii · Y. Nishise · J. Ito · H. Watanabe · K. Saito · S. Kawata
Department of Gastroenterology,
Yamagata University School of Medicine,
2-2-2 Iida-nishi,
Yamagata 990-9585, Japan
e-mail: tasaitoh@med.id.yamagata-u.ac.jp

H. Togashi
Health Administrative Center, Yamagata University,
Yamagata, Japan

within 24 weeks, leading to an improvement in the Child-Pugh score (Terai et al. 2006).

Although the transplantation of BMCs has been demonstrated to aid recovery from severe liver damage in vivo, details of the interaction of transplanted BMCs with hepatic stem cells in the liver have not been elucidated. We have previously found that BMC transplantation is successful in rats with severe liver injury, producing marked expression of mRNAs for *HGF* and *fibroblast growth factor* (*FGF*; Okumoto et al. 2006). In a liver environment in which hepatocyte proliferation is strongly inhibited, hepatic stem cells such as oval cells are induced and show differentiation toward a liver cell lineage, thus leading to liver regeneration (Shiota et al. 2000; Hu et al. 1993). The hypothesis that transplanted BMCs interact with hepatic stem cells and influence the subsequent proliferation and differentiation of stem cells in the injured liver has received considerable support, but so far, no study has investigated the interaction between BMCs and hepatic stem cells both in vitro and in vivo.

In the present study, we have developed an in vitro culture system for the co-culture of BMCs and an established epithelial hepatic stem cell line named hepatic stem-like cells (HSLCs). Using this system, we have investigated the proliferation and differentiation of HSLCs into the hepatocyte lineage with or without BMC co-culture. We have also detected a stimulating factor that is produced by interacting BMCs and that influences the hepatocyte differentiation of HSLCs.

Materials and methods

Characterization of hepatic epithelial stem-like cells

An established hepatic epithelial stem-like cell line derived from the healthy liver of an adult male Sprague-Dawley rat and designated HSLC (Nagai et al. 2002; Miura et al. 2003) was used. Among a number of liver epithelial cell lines that have been established (Grisham and Thorgeirsson 1997), the phenotypic properties of WB-344 cells and RLE cells are well documented (Grisham et al. 1993; Bisgaard et al. 1994). The significant phenotypic features common to these cells are positivity for both alpha-fetoprotein (AFP) and albumin and negativity for cytokeratin (CK) 19, indicating that the cells are not completely differentiated liver cells. The HSLCs used in this study have an immature liver cell phenotype with positive expression of AFP but are negative for albumin, CK19, and tyrosine aminotransferase (TAT). The cells expressing AFP probably originated from non-parenchymal cells of the normal adult liver, as described previously (Nagai et al. 2002). Although HSLCs share some phenotypic similarities with the other liver epithelial cells mentioned above, they do not express albumin, which is a marker of mature hepatocytes, suggesting that HSLCs are less mature than the other cell lines. HSLCs also exhibit the potential to differentiate into cells of the hepatocytic lineage and serve as stem-like cells for differentiation into hepatocytes in vitro (Hattori et al. 2010).

Isolation of BMCs

BMCs were obtained from 8-week-old male Sprague-Dawley rats by flushing their femurs with phosphate-buffered saline pH 7.2 (PBS) and then dispersed by passage through a 21-gauge needle. The cells were then filtered through a Cell Strainer (BD Biosciences, Bedford, Mass., USA) of mesh size 40 μm, and mononuclear cells were obtained by Lympholyte (Cedarlane, Ontario, Canada) gradient centrifugation and cultured in a monolayer.

Co-culture of BMCs and HSLCs

We established an in vitro co-culture system for BMCs and HSLCs, by using a 6-well culture plate in which the cells were contained in two chambers separated by a semi-permeable membrane (Transwell^{R}, Corning Coaster, Cambridge, Mass., USA; pore size: 0.4 μm), as shown in Fig. 1. The cells for use in the assay and the other cells for co-culture were plated in the lower and upper chambers, respectively. As a control, the cells for use in the assay were plated in the lower chamber, but no cells were plated in the upper chamber. The numbers of HSLCs and BMCs used in this culture were 5×10^4 and 2×10^5, respectively, as appropriate for a 72-h culture in order to avoid over 100% confluent growth of the cells on the culture plate. The cells were cultured for 72 h in Dulbecco's modified Eagle's medium/F12 (DMEM/F12; Invitrogen, Carlsbad, Calif., USA) containing 10% fetal bovine serum albumin, 100 U/ml penicillin, 100 μg/ml streptomycin, and 1 μl/ml insulin-transferrin-selenium (Invitrogen), at 37°C, in a humidified atmosphere containing 5% CO_2.

HSLC proliferation assay

Cell viability was determined by using the Premix WST-1 cell proliferation assay system (Takara Biochemicals, Tokyo, Japan). Briefly, after removal of the upper chamber containing the BMCs, 200 μl Premix WST-1 was added to the lower chamber containing the HSLCs, and cell proliferation was measured by the WST-1 assay after 72 h of incubation. The plates were incubated for 120 min at 37°C, and the absorbances at 450 nm and 620 nm were measured by using a Benchmark Plus microplate reader (Bio-Rad Laboratories, Hercules, Calif., USA). The assay was repeated eight times.

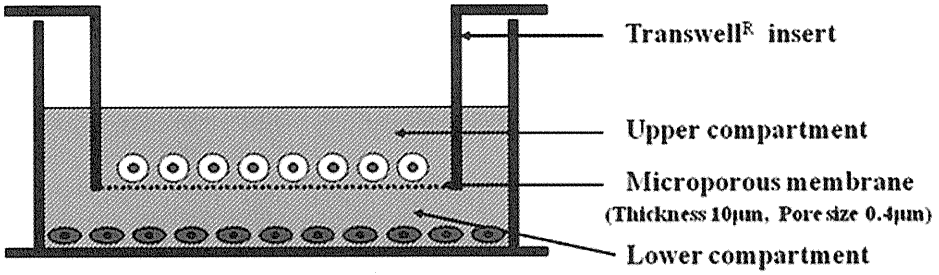

Fig. 1 Establishment of a system for co-culture of bone marrow cells (BMCs) with hepatic stem-like cells (HSLCs) by using a 6-well culture plate in which the cells were placed in two different chambers separated by a semi-permeable membrane (*a* experimental, *b* control)

Culture Condition	Upper compartment	Lower compartment
a	Co-culture cells	Cells for assay
b	—	Cells for assay

RNA extraction

Total cellular RNAs of HSLCs were extracted by using the Isogen kit (Wako Pure Chemical Industries, Osaka, Japan) in accordance with the manufacturer's instructions. Briefly, a sample was treated with 1 ml Isogen, and the solution was mixed with 0.2 ml chloroform. After centrifugation at 12,000*g* at 4°C for 15 min, the supernatant was transferred to a new tube and mixed with an equal volume of isopropanol to precipitate the RNA. Following centrifugation as described above, the pellet was washed with 70% ethanol, recentrifuged at 10,000*g* at 4°C for 5 min, air-dried, and then dissolved in RNase-free water. RNA concentrations were determined by ultraviolet spectrophotometry (UV-1200 spectrophotometer, Shimazu, Kyoto, Japan).

Detection of liver-specific mRNA expression in HSLCs by reverse transcription with the polymerase chain reaction

First-strand cDNAs were synthesized from 3 μg total RNA from HSLCs in a 21-μl reaction volume by using the SuperScript First-Strand Synthesis System for reverse transcription with the polymerase chain reaction (RT-PCR; Invitrogen) in accordance with the manufacturer's instructions. The cDNA (1 μl) was then amplified by PCR over 35 cycles including denaturation at 94°C for 1 min, annealing at 60°C for 1 min for *tryptophan 2,3-dioxygenase*, *AFP*, *TAT*, *albumin*, and *D-glyceraldehyde-3-phosphate dehydrogenase* (*GAPDH*) or at 56°C for 1 min for *fibroblast growth factor receptor 2* (*FGFR2*), and extension at 72°C for 1 min by using a Perkin-Elmer 9600 thermal cycler platform (Perkin-Elmer, Norwalk, Conn., USA). The primers used for PCR to detect mRNA expression were as follows: (1) *AFP* mRNA 5′-CACCATCGAGCTCGGCTATT-3′ and 5′-TGATGCAGAGCCTCCTGTTG-3′ (PCR product; 620 bp); (2) *albumin* mRNA 5′-ATACACCCAGAAAGCACCTC-3′ and 5′-CAGAGTGGAAGGTGAAGGTC-3′ (PCR product; 305 bp); (3) *tryptophan 2,3-dioxygenase* mRNA 5′-CAGCTGAGTACAGCGACAGC-3′ and 5′-TCTATGGAGGTAAGTGTCAG-3′ (PCR product; 330 bp); (4) *TAT* mRNA 5′-TGAACAGCACTACCACTGTG-3′ and 5′-AGGCATCCTCCGTCTTCTGC-3′ (PCR product; 380 bp); (5) *FGFR2* mRNA 5′-AACCAAATACCAAATCTCCCAACC-3′ and 5′-ATCTGTGTCGTCCTCGTCATCTCC-3′ (PCR product; 298 bp); (6) *GAPDH* mRNA as a control 5′-ATCACTGCCACTCAGAAGAAGAC-3′ and 5′-TGAGGGAGATGCACAGTGTT-3′ (PCR product; 580 bp).

Immunofluorescence staining for FGFR2 in HSLCs

The expression of FGFR2 was analyzed by indirect immunofluorescence staining. HSLCs were washed with PBS and fixed with cold acetone. The cells were then incubated with a primary antibody against FGFR2 (Santa Cruz Biotechnology, Santa Cruz, Calif., USA) diluted 1:100, at 4°C overnight. After being washed with PBS, the cells were incubated with fluorescein-isothiocyanate-conjugated rabbit anti-rabbit IgG (DAKO, Kyoto, Japan) at 4°C for 1 h and then observed by using a confocal laser scanning microscope (LSM-510 Meta, Carl Zeiss, Germany).

DNA microarray analysis of BMCs co-cultured with HSLCs

Total RNA of the BMCs co-cultured with HSLCs were extracted by using the method described above and subjected to DNA microarray analysis (Rat Genome 230 2.0 Array, Takara Biochemicals). BMCs cultured alone

were used as a control. GeneChip analyses were carried out by Takara Custom Services (Takara Biochemicals). The hybridization signals were analyzed by using GeneChip operating software, version 1.4 (Takara Biochemicals).

Quantitation of FGF2 mRNA expression in BMCs

The methods used for RNA extraction and cDNA amplification were the same as those described above. To quantify the level of *FGF2* mRNA in BMCs co-cultured with HSLCs and in those cultured alone, we performed real-time PCR by using the LightCycler Quick System 350S (Roche Diagnostics, Tokyo, Japan). The RT reaction was subjected to PCR amplification by using LightCycler Fast Start DNA Master SYBR Green I (Roche Diagnostics, Tokyo, Japan) in accordance with the manufacturer's instructions. The amplification program employed was 95°C for 1 min followed by 40 cycles consisting of 95°C for 1 s, 62°C for 5 s, and 72°C for 10 s. The primers for the detection of *FGF2* mRNA in the real-time PCR were 5′-AACCAAATACCAAATCTCC-CAACC-3′ and 5′-ATCTGTGTCGTCCTCGTCATCTCC-3′. The assay was repeated three times.

Culture of HSLCs with recombinant FGF2

HSLCs were cultured with recombinant FGF2 (R&D Systems, Minneapolis, Minn., USA) at a concentration of 0, 10, or 20 ng/ml in culture medium containing DMEM/F12, 10% fetal bovine serum albumin, 100 U/ml penicillin, 100 μg/ml streptomycin, and 1 μl/ml insulin-transferrin-selenium at 37° C in a humidified atmosphere containing 5% CO_2. The above-described methods were employed to check cell proliferation every day after 1–6 days of culture, and the differentiation of HSLCs into the hepatocyte lineage was analyzed on culture day 3. Differentiation of HSLCs that had been pre-treated with anti-FGFR2 antibody (Santa Cruz Biotechnology) at a concentration of 2 μg/ml into the hepatocyte lineage was also examined on culture day 3.

Statistical analysis

Statistical analyses were performed by using Student's *t*-test and one-way analysis of variance, and differences at $P<0.05$ were considered to be significant.

Results

Proliferation and liver-specific mRNA expression in HSLCs co-cultured with BMCs

The viability of HSLCs, in terms of their proliferation ability, was significantly higher for those co-cultured with BMCs than for those cultured without BMCs (1.19 ±0.08 nm vs. 0.48±0.08 nm, mean ± SD; $P<0.001$; Fig. 2). Expression of mRNA for *albumin* and *tryptophan-2,3-dioxygenase* was detected in HSLCs co-cultured with BMCs on culture day 3, but no such mRNA expression was observed in HSLCs cultured without BMCs (Fig. 3). The morphology of HSLCs before culture with BMCs and those on day 3 of culture with BMCs is shown in Fig. 4a, b, respectively. Thus BMCs induced both the proliferation and differentiation of HSLCs into the hepatocyte lineage in vitro.

DNA microarray analysis of BMCs cultured with HSLCs

To determine the upregulation of gene expression in BMCs co-cultured with HSLCs, the gene expression profile of co-cultured BMCs in comparison with that of BMCs cultured alone was investigated by DNA microarray analysis. A scatter plot of the DNA data showed that the gene expression profiles of the two sets of cells differed (Fig. 5). Upregulated genes that could potentially affect the proliferation and differentiation of HSLCs are shown in Table 1. The highest degree of upregulation was exhibited by *FGF2*, its mRNA level being 7.46-times higher in BMCs co-cultured with HSLCs than that in BMCs cultured alone.

Expression of FGF2 mRNA in BMCs co-cultured with HSLCs

Real-time PCR was applied to test the level of cellular *FGF2* mRNA expression in BMCs cultured with or without

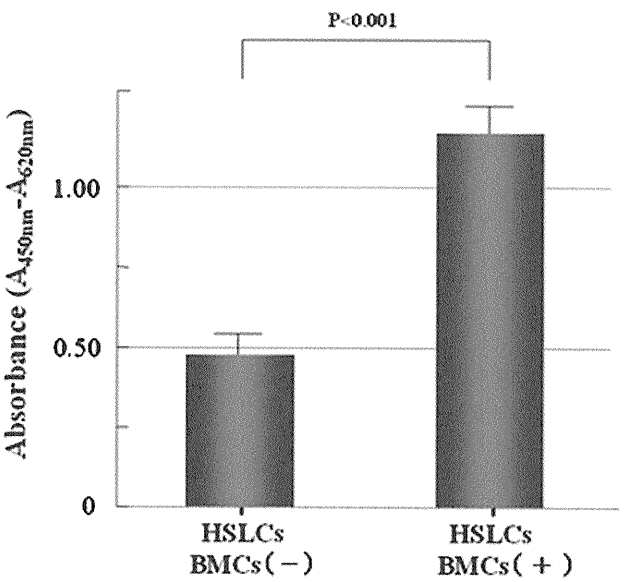

Fig. 2 Proliferation of HSLCs cultured with (+) or without (-) BMCs. Proliferation was measured after 72 h of culture. The WST-1 assay was repeated eight times

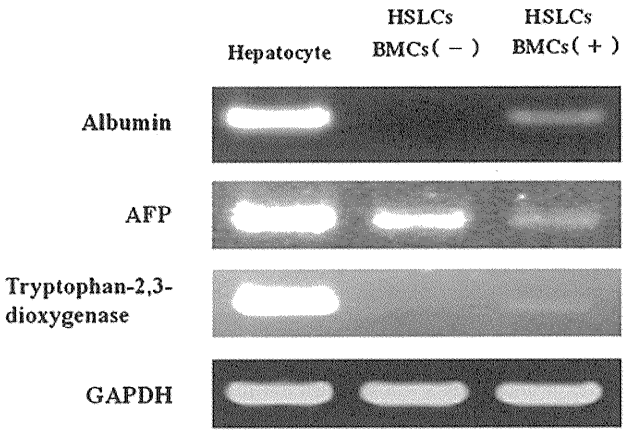

Fig. 3 Analysis of mRNA expression by reverse transcription with the polymerase chain reaction (RT-PCR) for liver-specific proteins including albumin, alpha-fetoprotein (*AFP*), and tryptophan-2,3-dioxygenase in HSLCs cultured with (+) or without (-) BMCs on culture day 3 (*GAPDH* D-glyceraldehyde-3-phosphate dehydrogenase, control)

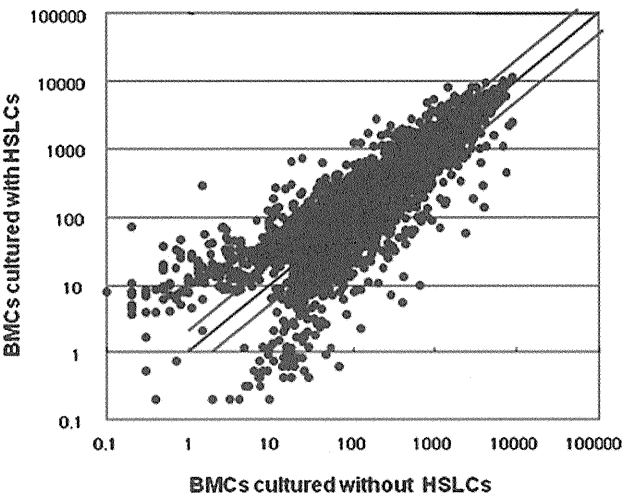

Fig. 5 Gene expression profile of BMCs cultured with HSLCs in comparison with BMCs cultured alone

HSLCs. On culture day 3, the expression of *FGF2* mRNA was significantly higher in BMCs co-cultured with HSLCs than in BMCs cultured alone ($1.25\pm1.02\times10^{10}$copy/ml vs $3.41\pm1.02\times10^{8}$ copy/ml; $P<0.05$; Fig. 6). Thus, the expression of *FGF2* mRNA was shown to be enhanced in BMCs when they were cultured with HSLCs.

FGFR2 expression in HSLCs

To investigate whether FGF2 is functional in HSLCs, the expression of its receptor in these cells was analyzed. Expression of *FGF receptor 2* (*FGFR2*) mRNA was detectable in HSLCs by RT-PCR. Immunofluorescence staining for FGFR2 protein demonstrated positive expression on the cell membrane of all HSLCs detectable in the monolayer culture (Fig. 7).

FGF2 stimulates hepatocyte differentiation of HSLCs

HSLCs were exposed to 0, 10, and 20 ng/ml FGF2 in culture, and proliferation was measured every day after 1–6 days of incubation in 96-well plates by the WST-1 assay. HSLCs showed no difference in proliferation among the three groups cultured with different concentrations of FGF2 for 6 days (Fig. 8). Using RT-PCR, we examined the expression of mRNA for liver-specific proteins in HSLCs cultured with FGF2. On culture day 3, the expression of mRNA for both *albumin* and *TAT* was detectable in HSLCs cultured with FGF2 at concentrations of 10 and 20 ng/ml (Fig. 9). No such expression was evident in cells cultured without FGF2 or in cells pre-treated with anti-FGFR2 antibody. These data indicate that FGF2, whose mRNA expression increases in BMCs co-cultured with HSLCs, is

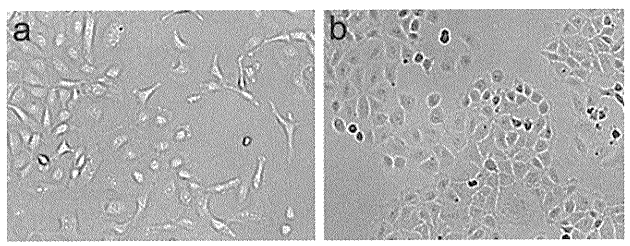

Fig. 4 Morphology of HSLCs before culture with BMCs (**a**) and those on day 3 of culture with BMCs (**b**). Magnification ×100

Table 1 Upregulated genes in BMCs possibly affecting proliferation and differentiation of HSLCs (*EGF* epidermal growth factor)

Function	Accession no.	Gene name (abbreviation/ alternative name)	Ratio
Growth factor	BF284027	Fibroblast growth factor 2 (FGF2)	7.46
	NM_021689	Epiregulin	6.96
	NM_012827	Bone morphogenetic protein 4	5.28
	AF140232	S100 calcium-binding protein A6 (calcylin)	4.92
	NM_012945	Heparin-binding EGF-like growth factor	3.25
	AI175732	Vascular endothelial growth factor	2.83
	NM_017104	Colony-stimulating factor 3 (G-CSF)	2.64
	AB001382	Secreted phosphoprotein 1 (osteopontin)	2.30
	U00620	Colony stimulating factor 2 (GM-CSF)	2.30
	BE100812	Platelet-derived growth factor-alpha	2.00